

## Reactivity Study of a Hydroperoxodicopper(II) Complex: Hydroxylation, Dehydrogenation, and Ligand Cross-Link Reactions

Lei Li, Amy A. Narducci Sarjeant, and Kenneth D. Karlin\*

Department of Chemistry, The Johns Hopkins University, Baltimore, Maryland 21218

Received April 8, 2006

Employing a binucleating phenol-containing ligand PD'OH, a  $\mu$ -phenoxo- $\mu$ -hydroperoxo dicopper(II) complex  $[\text{Cu}^{\text{II}}_2(\text{PD}'\text{O}^-)(\text{OOH})(\text{RCN})_2](\text{ClO}_4)_2$  (**1**, R = CH<sub>3</sub>, CH<sub>3</sub>CH<sub>2</sub> or C<sub>6</sub>H<sub>5</sub>CH<sub>2</sub>;  $\lambda_{\text{max}} = 407$  nm;  $\nu_{(\text{O}-\text{O})} = 870$  cm<sup>-1</sup>; *J. Am. Chem. Soc.* **2005**, *127*, 15360) is generated by reacting a precursor dicopper(I) complex  $[\text{Cu}^{\text{I}}_2(\text{PD}'\text{OH})(\text{CH}_3\text{CN})_2](\text{ClO}_4)_2$  (**2**) with O<sub>2</sub> in nitrile solvents at -80 °C. Species **1** is unable to oxidize externally added substrates, for instance, PPh<sub>3</sub>, 2,4-*tert*-butylphenol, or 9,10-dihydroanthracene. However, upon thermal decay, it hydroxylates copper-bound organocyanides (e.g., benzylcyanide), leading to the corresponding aldehyde while releasing cyanide. This chemistry mimics that known for the copper enzyme dopamine- $\beta$ -monooxygenase. The thermal decay of **1** also leads to a product  $[\text{Cu}^{\text{II}}_3(\text{L}'')_2(\text{Cl}^-)_2](\text{PF}_6)_2$  (**6**); its X-ray structure reveals that L'' is a Schiff base-containing ligand which apparently derives from both oxidative N-dealkylation and then oxidative dehydrogenation of PD'OH; the chloride presumably derives from the CH<sub>2</sub>Cl<sub>2</sub> solvent. With an excess of PPh<sub>3</sub> added to **1**, a binuclear Cu(I) complex  $[\text{Cu}^{\text{I}}_2(\text{L}')(\text{PPh}_3)_2](\text{ClO}_4)_2$  (**5**) with a cross-linked PD'OH ligand L' has also been identified and crystallographically and chemically characterized. The newly formed C–O bond and an apparent  $k_{\text{H}}/k_{\text{D}} = 2.9 \pm 0.2$  isotope effect in the benzylcyanide oxidation reaction suggest a common ligand-based radical forms during compound **1** thermal decay reactions. A di- $\mu$ -hydroxide-bridged tetranuclear copper(II) cluster compound  $\{[\text{Cu}^{\text{II}}_2(\text{PD}'\text{O}^-)(\text{OH}^-)]_2\}(\text{ClO}_4)_4$  (**8**) has also been isolated following warming of **1**. Its formation is consistent with the generation of  $[\text{Cu}^{\text{II}}_2(\text{PD}'\text{O}^-)(\text{OH}^-)]^{2+}$ , with dimerization a reflection of the large Cu...Cu distance and thus the preference for not having a second bridging ligand atom (in addition to the phenolate O) for dicopper(II) ligation within the PD'O<sup>-</sup> ligand framework.

### Introduction

Copper-complex-mediated activation of dioxygen, i.e., binding of O<sub>2</sub> to copper ion and generation of species capable of substrate oxidation/oxygenation reactions, is of considerable interest. For instance, Porco and co-workers recently applied copper–dioxygen chemistry to effect copper-mediated enantioselective oxidation chemistry in the synthesis of natural product azaphilones.<sup>1</sup> Further, copper/O<sub>2</sub> reactivity has relevance to biology and copper enzyme oxygenases and oxidases.<sup>2–8</sup>

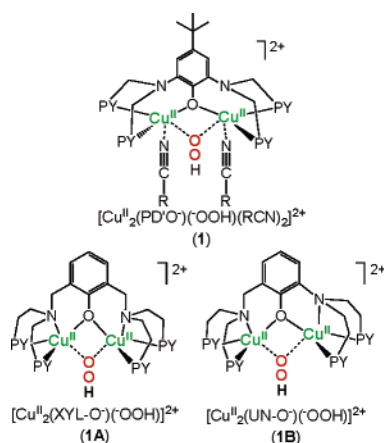
Copper hydroperoxides (Cu<sub>n</sub>–OOH,  $n = 1, 2$ ) are one type of species which have drawn attention for their chemical reactions and biological relevance. A mononuclear Cu<sup>II</sup>–OOH species was at one time suggested to be the active species to initiate the hydrogen atom abstraction reaction chemistry observed in dopamine- $\beta$ -monooxygenase (D $\beta$ M) and peptidylglycine  $\alpha$ -hydroxylating monooxygenase (PHM),<sup>5</sup> although recent studies rather suggest a copper(II)–superoxide species is relevant.<sup>4,9–11</sup> A Cu<sup>I</sup>Cu<sup>II</sup>–OOH species has been implied to form as one of the intermediates during the O<sub>2</sub> reaction catalyzed by a trinuclear (Cu<sub>3</sub>) active site metal cluster in multicopper oxidases (reducing O<sub>2</sub> to water) such

\* To whom correspondence should be addressed. E-mail: karlin@jhu.edu.

- (1) Zhu, J. L.; Grigoriadis, N. P.; Lee, J. P.; Porco, J. A. *J. Am. Chem. Soc.* **2005**, *127*, 9342–9343.
- (2) Solomon, E. I.; Sundaram, U. M.; Machonkin, T. E. *Chem. Rev.* **1996**, *96*, 2563–2606.
- (3) Lieberman, R. L.; Rosenzweig, A. C. *Nature* **2005**, *434*, 177–82.
- (4) Prigge, S. T.; Eipper, B. A.; Mains, R. E.; Amzel, L. M. *Science* **2004**, *304*, 864–867.
- (5) Klinman, J. P. *Chem. Rev.* **1996**, *96*, 2541–2561.
- (6) Lewis, E. A.; Tolman, W. B. *Chem. Rev.* **2004**, *104*, 1047–1076.

- (7) Hatcher, L. Q.; Karlin, K. D. *J. Biol. Inorg. Chem.* **2004**, *9*, 669–683.
- (8) Mirica, L. M.; Ottenwaelder, X.; Stack, T. D. P. *Chem. Rev.* **2004**, *104*, 1013–1045.
- (9) Chen, P.; Solomon, E. I. *J. Am. Chem. Soc.* **2004**, *126*, 4991–5000.
- (10) Evans, J. P.; Ahn, K.; Klinman, J. P. *J. Biol. Chem.* **2003**, *278*, 49691–49698.
- (11) Klinman, J. P. *J. Biol. Chem.* **2006**, *281*, 3013–3016.

Chart 1



as laccase.<sup>12,13</sup> In biomimetic model compound studies, two types of copper–hydroperoxide species have been produced to date, dinuclear  $\mu$ -1,1-hydroperoxo-dicopper(II)<sup>14–19</sup> and mononuclear hydroperoxo-copper(II) complexes.<sup>20–29</sup>

Here, we present a full report on the synthesis, characterization, and reactivity of a  $\mu$ -1,1-hydroperoxo dicopper(II) species  $[\text{Cu}^{\text{II}}_2(\text{PD}'\text{O}^-)(-\text{OOH})(\text{RCN})_2](\text{ClO}_4)_2$  (**1**,  $\text{R} = \text{CH}_3, \text{CH}_3\text{CH}_2, \text{or } \text{C}_6\text{H}_5\text{CH}_2$ , Chart 1), possessing rather novel structural and reactivity characteristics: As we recently described,<sup>30</sup> upon thermal decay, this  $\text{Cu}^{\text{II}}_2\text{-OOH}$  species

hydroxylates the nitrile solvent which is present, subsequently releasing aldehyde and cyanide [i.e.,  $\text{Cu}^{\text{II}}_2(-\text{O}_2\text{H}) + \text{RCH}_2\text{-CN} \rightarrow \text{RCHO} + \text{Cu}^{\text{II}}_2(-\text{CN}) + \text{H}_2\text{O}$ ]. This reaction is of biological interest as  $D\beta M$  catalyzes a similar reaction.<sup>31</sup> We find that **1** possesses an extensive chemistry, and in this report, we detail other reactions observed. The isolation and X-ray structural characterization have been accomplished for derivatives of **1** which have undergone oxidations on the binucleating ligand  $\text{PD}'\text{O}^-$ . The results are also compared and contrasted to the chemistry and reactions of structural analogues  $[\text{Cu}^{\text{II}}_2(\text{XYL}-\text{O}^-)(-\text{OOH})]^{2+}$  (**1A**) and  $[\text{Cu}^{\text{II}}_2(\text{UN}-\text{O}^-)(-\text{OOH})]^{2+}$  (**1B**) (Chart 1).

## Experimental Section

**Materials and Methods.** Unless otherwise stated, all solvents and chemicals used were of commercially available analytical grade. Dioxygen was dried by passing through a short column of supported  $\text{P}_{4010}$  (Aquasorb, Mallinckrodt). Propionitrile was distilled over  $\text{CaH}_2$ , and diethyl ether, acetonitrile, and methylene chloride were used after passing them through a 60-cm-long column of activated alumina (Innovative Technologies, Inc.) under  $\text{N}_2$ . The preparation and handling of air-sensitive compounds were performed under an argon atmosphere using standard Schlenk techniques or in an MBraun Labmaster 130 inert atmosphere ( $<1$  ppm  $\text{O}_2$ ,  $<1$  ppm  $\text{H}_2\text{O}$ ) drybox filled with nitrogen. Deoxygenation of solvents was effected by either repeated freeze/pump/thaw cycles or bubbling with argon for 30–45 min. Electron paramagnetic resonance (EPR) spectra were recorded on a Bruker EMX spectrometer controlled with a Bruker ER 041 X G microwave bridge operating at X-band ( $\sim 9.4$  GHz). Low-temperature EPR measurements were carried out via either a continuous-flow liquid-helium cryostat and ITC503 temperature controller made by Oxford Instruments, Inc. or a liquid-nitrogen finger dewar. Elemental analyses were performed by Quantitative Technologies, Inc. (QTI, Whitehouse, NJ) or Desert Analytics (Tucson, AZ).  $^1\text{H}$  NMR spectra were recorded at 300 MHz on a Bruker AMX-300 instrument. Chemical shifts were reported as  $\delta$  values relative to an internal standard ( $\text{Me}_4\text{Si}$ ) and the residual solvent proton peak. All GC/MS experiments were carried out and recorded using a Shimadzu GC-17A/GCMS0QP5050 gas chromatograph/mass spectrometer. All GC experiments were carried out and recorded using a Hewlett-Packard 5890 Series II gas chromatograph.

**UV–Vis Experiments.** Room-temperature UV–vis spectra were recorded with a Varian Cary-50 spectrophotometer. Low-temperature UV–vis spectra were recorded on a Hewlett-Packard Model 8453A diode array spectrophotometer equipped with a two-window quartz H. S. Martin Dewar filled with cold MeOH (25 to  $-85$  °C) maintained and controlled by a Neslab VLT-95 low temp circulator. Spectrophotometer cells used were made by Quark Glass with column and pressure/vacuum side stopcock and 2 mm path length. Molecular  $\text{O}_2$  was bubbled into reaction solutions via an 18-gauge, 24-in.-long stainless steel syringe needle.

**Ligand  $\text{PD}'\text{OH}$ ,  $[\text{Cu}^{\text{II}}_2(\text{PD}'\text{OH})(\text{CH}_3\text{CN})_2](\text{ClO}_4)_2$  (**2**),  $[\text{Cu}^{\text{II}}_2(\text{PD}'\text{OH})(\text{BzCN})_2](\text{PF}_6)_2$  ( $\text{BzCN} = \text{Benzylcyanide}$ ) and Generation of  $[\text{Cu}^{\text{II}}_2(\text{PD}'\text{O}^-)(-\text{OOH})(\text{RCN})_2]^{2+}$  (**1**).** These syntheses or manipulations were carried out as previously described.<sup>30,32</sup> **Caution:** Although we encountered no problems by using perchlorate

- (12) Rulisek, L.; Solomon, E. I.; Ryde, U. *Inorg. Chem.* **2005**, *44*, 5612–28.
- (13) Kataoka, K.; Kitagawa, R.; Inoue, M.; Naruse, D.; Sakurai, T.; Huang, H. W. *Biochemistry* **2005**, *44*, 7004–7012.
- (14) Karlin, K. D.; Ghosh, P.; Cruse, R. W.; Farooq, A.; Gultneh, Y.; Jacobson, R. R.; Blackburn, N. J.; Strange, R. W.; Zubieta, J. *J. Am. Chem. Soc.* **1988**, *110*, 6769–6780.
- (15) Murthy, N. N.; Mahroof-Tahir, M.; Karlin, K. D. *Inorg. Chem.* **2001**, *40*, 628–635.
- (16) Mahroof-Tahir, M.; Murthy, N. N.; Karlin, K. D.; Blackburn, N. J.; Shaikh, S. N.; Zubieta, J. *Inorg. Chem.* **1992**, *31*, 3001–3003.
- (17) Root, D. E.; Mahroof-Tahir, M.; Karlin, K. D.; Solomon, E. I. *Inorg. Chem.* **1998**, *37*, 4838–4848.
- (18) Itoh, K.; Hayashi, H.; Furutachi, H.; Matsumoto, T.; Nagatomo, S.; Tosha, T.; Terada, S.; Fujinami, S.; Suzuki, M.; Kitagawa, T. *J. Am. Chem. Soc.* **2005**, *127*, 5212–5223.
- (19) Battaini, G.; Monzani, E.; Perotti, A.; Para, C.; Casella, L.; Santagostini, L.; Gullotti, M.; Dillinger, R.; Nather, C.; Tucek, F. *J. Am. Chem. Soc.* **2003**, *125*, 4185–4188.
- (20) Wada, A.; Harata, M.; Hasegawa, K.; Jitsukawa, K.; Masuda, H.; Mukai, M.; Kitagawa, T.; Einaga, H. *Angew. Chem., Int. Ed.* **1998**, *37*, 798–799.
- (21) Yamaguchi, S.; Masuda, H. *Adv. Mater. Sci. Technol.* **2005**, *6*, 34–47.
- (22) Koder, M.; Kita, T.; Miura, I.; Nakayama, N.; Kawata, T.; Kano, K.; Hirota, S. *J. Am. Chem. Soc.* **2001**, *123*, 7715–7716.
- (23) Fujii, T.; Naito, A.; Yamaguchi, S.; Wada, A.; Funahashi, Y.; Jitsukawa, K.; Nagatomo, S.; Kitagawa, T.; Masuda, H. *Chem. Commun.* **2003**, 2700–2701.
- (24) Yamaguchi, S.; Nagatomo, S.; Kitagawa, T.; Funahashi, Y.; Ozawa, T.; Jitsukawa, K.; Masuda, H. *Inorg. Chem.* **2003**, *42*, 6968–6970.
- (25) Yamaguchi, S.; Wada, A.; Nagatomo, S.; Kitagawa, T.; Jitsukawa, K.; Masuda, H. *Chem. Lett.* **2004**, *33*, 1556–1557.
- (26) Osako, T.; Nagatomo, S.; Tachi, Y.; Kitagawa, T.; Itoh, S. *Angew. Chem., Int. Ed.* **2002**, *41*, 4325–4328.
- (27) Ohtsu, H.; Itoh, S.; Nagatomo, S.; Kitagawa, T.; Ogo, S.; Watanabe, Y.; Fukuzumi, F. *Inorg. Chem.* **2001**, *40*, 3200–3207.
- (28) Ohtsu, H.; Itoh, S.; Nagatomo, S.; Kitagawa, T.; Ogo, S.; Watanabe, Y.; Fukuzumi, F. *Chem. Commun.* **2000**, 1051–1052.
- (29) Chen, P.; Fujisawa, K.; Solomon, E. I. *J. Am. Chem. Soc.* **2000**, *122*, 10177–10193.
- (30) Li, L.; Narducci Sarjeant, A. A.; Vance, M. A.; Zakharov, L. N.; Rheingold, A. L.; Solomon, E. I.; Karlin, K. D. *J. Am. Chem. Soc.* **2005**, *127*, 15360–15361.

(31) Baldoni, J. M.; Villafranca, J. J. *J. Biol. Chem.* **1980**, *255*, 8987–8990.

(32) Li, L.; Karlin, K. D.; Rokita, S. E. *J. Am. Chem. Soc.* **2005**, *127*, 520–521.

salts or in the preparation and handling of peroxide and hydroperoxide complexes (experimental details given below), appropriate precautions should be taken.

**General Procedure for Substrate Oxidation Studies by  $[\text{Cu}^{\text{II}}_2(\text{PD}'\text{O}^-)(-\text{OOH})(\text{EtCN})_2](\text{ClO}_4)_2$  (**1**).** Complex **2** (48 mg, 0.05 mmol) was dissolved in 8 mL of  $\text{O}_2$ -free propionitrile (under Ar), giving a bright yellow solution. This was cooled to  $-80^\circ\text{C}$  in a dry ice/acetone bath, and  $\text{O}_2$  was slowly (to minimize warming) bubbled through a long syringe needle into the reaction solution until full formation of the corresponding green hydroperoxodicopper(II) complex (**1**) occurred ( $\sim 1$  min). At  $-80^\circ\text{C}$ , 2 mL of propionitrile solution containing 1–2 equiv of substrates was added dropwise to this hydroperoxide solution via syringe. Any  $\text{O}_2$  remaining was removed by purging argon through the solution. The resulting solution was then allowed to decay by warming to ambient temperature. A reddish-brown solution was obtained after 2 h. Diethyl ether (100 mL) was added to this solution to precipitate the resulting copper complex. The mixture was filtered, the supernatant was analyzed by gas chromatography (GC), and the yield was calculated by comparing the corresponding product signal with a decane signal added as an internal standard.

The following GC conditions were used.

**$\text{PPh}_3$  Oxidation and 2,4-Di-*tert*-butylphenol Oxidation.** Initial oven temperature,  $120^\circ\text{C}$ ; initial time, 2 min; final oven temperature,  $220^\circ\text{C}$ ; final time, 7 min; gradient rate,  $40^\circ\text{C}/\text{min}$ ; flow rate, 16 mL/min; injector port temperature,  $250^\circ\text{C}$ ; detector temperature,  $280^\circ\text{C}$ .

**9,10-Dihydroanthracene Oxidation.** Oven temperature,  $200^\circ\text{C}$ ; flow rate, 50 mL/s; injection temperature,  $250^\circ\text{C}$ ; detection temperature,  $280^\circ\text{C}$ .

**$[\text{Cu}^{\text{II}}_2(\text{PD}'\text{O}^-)(-\text{OOH})_2]^+$  (**4**).**  $[\text{Cu}^{\text{II}}_2(\text{PD}'\text{O}^-)(\text{H}_2\text{O})_2]^{3+}$  (**3**) (31 mg, 0.03 mmol) was dissolved in 8 mL of propionitrile, giving a clear blue solution. This was cooled to  $-80^\circ\text{C}$  in a dry ice/acetone bath, and 2 mL of propionitrile solution containing 100 equiv of  $\text{H}_2\text{O}_2$  (102 mg, 3 mmol) were added dropwise. Almost no solution color change was observed. However, subsequent dropwise addition of 1 mL of propionitrile solution containing 100 equiv of triethylamine (303 mg, 3 mmol) immediately caused a color change to a yellowish-green. UV-vis spectra revealed this species to possess a strong charge-transfer band at 362 nm ( $\epsilon = 2200 \text{ M}^{-1} \text{ cm}^{-1}$ ).

**Quantitative Determination of  $\text{H}_2\text{O}_2$  Formed upon Protonation of **1**.** To a solution of 0.3 mmol of **1** prepared in situ (EtCN,  $-80^\circ\text{C}$ ) were added 10 equiv (3 mmol) of  $\text{HPF}_6/\text{Et}_2\text{O}$ . The green solution instantly turned blue. The reaction mixture was stirred for 15 min, and then diethyl ether (60 mL) was added to precipitate the metal complex product(s). The precipitate was allowed to settle, and the clear supernatant solution was transferred with a cannula to a flask containing a solution of KI (1.0 g) in a degassed mixture of distilled water (20 mL) and acetic acid (10 mL). The blue precipitate was washed with  $\text{O}_2$ -free ether (30 mL), and the supernatant was again transferred to the KI solution. The yellow KI mixture was stirred for 10 min at room temperature and then titrated by 0.05 N  $\text{Na}_2\text{S}_2\text{O}_3$  solution until it became colorless. The yield of  $\text{H}_2\text{O}_2$  formed calculated from the amount of 0.05 N  $\text{Na}_2\text{S}_2\text{O}_3$  solution consumed was found to be 21% (average of four determinations)

**$[\text{Cu}^{\text{II}}_2(\text{L}')(\text{PPh}_3)_2](\text{ClO}_4)_2$  (**5**,  $\text{L}' = \text{Cross-Linked PD}'\text{OH}$  Ligand).** To a solution of 0.1 mmol of **1** prepared in situ (EtCN,  $-80^\circ\text{C}$ ),  $\text{PPh}_3$  (105 mg, 0.4 mmol) in 4 mL of EtCN was added dropwise. After excess  $\text{O}_2$  was removed by purging with argon for 15 min, the solution was allowed to warm to ambient temperature. A red solution with UV absorption at 460 nm was obtained. Addition of

100 mL  $\text{O}_2$ -free diethyl ether afforded a reddish-brown colored precipitate. The precipitate was dried under vacuum overnight, giving a powder which was recrystallized under argon from  $\text{CH}_3\text{CN}/\text{Et}_2\text{O}$  to give 25 mg (20%) of orange-colored product.  $^1\text{H}$  NMR ( $\text{CD}_3\text{CN}$ , 300 MHz):  $\delta$  0.95 (s, 9H), 4.39 (s, br, 4H), 4.75 (s, br, 2H), 6.47 (s, 1H), 6.69 (s, 1H), 7.02 (s, 1H), 7.17–7.39 (m, 30H), 7.48–7.65 (m, 8H), 7.82–7.97 (m, 4H), 8.17–8.33 (m, 4H); UV-vis: (MeCN) 339 (sh,  $7900 \text{ M}^{-1} \text{ cm}^{-1}$ ); Anal. Calcd for ( $\text{C}_{70}\text{H}_{64}\text{Cl}_2\text{Cu}_2\text{N}_6\text{O}_9\text{P}_2$ ): C, 60.34; H, 4.63; N, 6.03. Found: C, 60.92; H, 4.88; N, 5.70.

**Isolation of the Cross-linked Ligand  $\text{L}'$  and  $\text{O}=\text{PPh}_3$  from Decomposition Products of **1**.** To a solution of 0.2 mmol of **1** prepared in situ (EtCN,  $-80^\circ\text{C}$ ),  $\text{PPh}_3$  (525 mg, 2 mmol) in 8 mL of EtCN solution was added dropwise. After removal of excess  $\text{O}_2$  by purging with argon for 15 min, this solution was allowed to warm to ambient temperature. An orange-colored solution was obtained. Addition of KCN (260 mg, 4 mmol) in aqueous solution (10 mL) along with 20 mL of  $\text{CH}_2\text{Cl}_2$  afforded a yellow methylene chloride layer and colorless aqueous solution.<sup>33</sup> The products in the  $\text{CH}_2\text{Cl}_2$  layer were separated and purified by column chromatography (silica gel). Elution with ethyl acetate followed by ethyl acetate/methanol (10:1) yielded  $\text{O}=\text{PPh}_3$  (36 mg, 65%,  $R_f = 0.6$ , silica, ethyl acetate) and the three-armed modified PD'OH product  $\text{L}'$  (65 mg, 60%) as a brown-yellow oil, ( $R_f = 0.30$ , silica gel, ethyl acetate/methanol = 10:1).  $^1\text{H}$  NMR ( $\text{CDCl}_3$ , 300 MHz):  $\delta$  1.16 (s, 9H), 4.37 (s, 4H), 4.56 (s, 2H), 6.37 (s, 1H), 6.60 (s, 1H), 7.02–7.05 (m, 4H), 7.12–7.15 (m, 1H), 7.36–7.41 (m, 2H), 7.42–7.46 (m, 1H), 7.60–7.66 (m, 1H), 8.45–8.50 (m, 2H), 8.58–8.62 (m, 1H). Mass ( $\text{M} + \text{Na}^+$ ): 476.

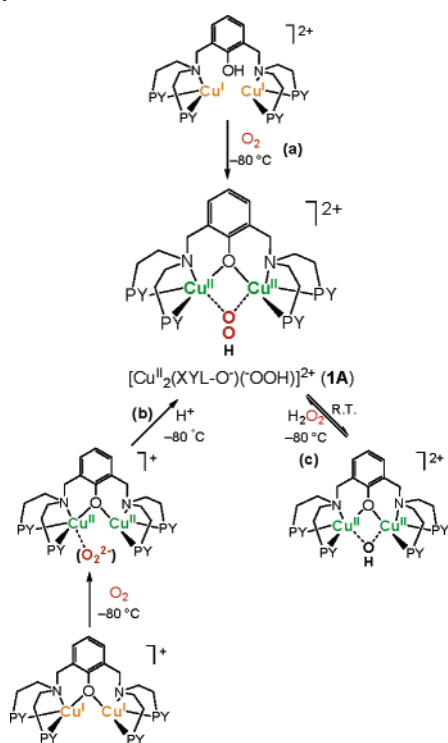
**$[\text{Cu}^{\text{II}}_3(\text{L}'')_2(\text{Cl}^-)_2](\text{PF}_6)_2$  (**6**,  $\text{L}'' = \text{Schiff Base-Containing Ligand}$ ).** Complex  $[\text{Cu}^{\text{II}}_2(\text{PD}'\text{OH})(\text{BzCN})_2](\text{PF}_6)_2$  (60 mg, 0.054 mmol) was dissolved in 2 mL of  $\text{O}_2$ -free  $\text{PhCH}_2\text{CN}/\text{CH}_2\text{Cl}_2$  (1:4) under an argon atmosphere, and the yellow solution was cooled to  $-80^\circ\text{C}$  in a dry ice/acetone bath. Dioxygen was gently bubbled through this solution for  $\sim 1$  min to enable complete formation of **1**. Since this is not very stable in the solvent mixture even at  $-80^\circ\text{C}$ , the solution was quickly purged with argon for  $\sim 2$  min to remove the excess  $\text{O}_2$  left in the solution and then warming to room temperature was allowed to occur. After 24 h, red crystals of **6** suitable for X-ray diffraction were obtained. Anal. Calcd for ( $\text{C}_{56}\text{H}_{56}\text{Cl}_2\text{Cu}_3\text{F}_{12}\text{N}_{10} \text{O}_2\text{P}_2$ ) $\cdot\text{CH}_2\text{Cl}_2$ : C, 44.53; H, 3.80; N, 9.11. Found: C, 44.22; H, 3.43; N, 8.76; UV-vis (MeCN,  $\lambda_{\text{max}}$ , nm): 460 ( $\epsilon = 18000 \text{ M}^{-1} \text{ cm}^{-1}$ ); IR (Nujol;  $\text{cm}^{-1}$ ) 1609 (HC=N); 843 ( $\text{PF}_6^-$ ); Magnetic Moment:  $2.7 \pm 0.1 \mu_{\text{B}}$  per trinuclear complex (as determined by the Evans NMR method in  $\text{CD}_3\text{CN}$ ).<sup>34</sup>

**Determination of the Yield of  $[\text{Cu}^{\text{II}}_3(\text{L}'')_2(\text{Cl}^-)_2](\text{PF}_6)_2$  (**6**).**  $[\text{Cu}^{\text{II}}_2(\text{PD}'\text{OH})(\text{BzCN})_2](\text{PF}_6)_2$  (60 mg, 0.054 mmol) was dissolved in 6 mL of  $\text{O}_2$ -free  $\text{PhCH}_2\text{CN}/\text{CH}_2\text{Cl}_2$  (1:4) under an argon atmosphere, and the yellow solution was cooled to  $-80^\circ\text{C}$  in a dry ice/acetone bath. Dioxygen was slowly (to minimize warming) bubbled through this solution ( $\sim 1$  min) to enable complete formation of **1**. The solution was quickly purged with argon for  $\sim 2$  min to remove the excess  $\text{O}_2$  left in the solution, followed by warming to ambient temperature. Addition of 100 mL of  $\text{O}_2$ -free diethyl ether afforded a reddish-brown colored precipitate. The precipitate was dried under vacuum overnight to give a red powder (48 mg). The yield of **6** was determined to be 56% by comparison of the UV-vis absorption of 1 mg of this red powder with pure complex as obtained by crystallization (see above).

(33) Sanyal, I.; Ghosh, P.; Karlin, K. D. *Inorg. Chem.* **1995**, *34*, 3050–3056.

(34) Evans, D. F.; James, T. A. *J. Chem. Soc., Dalton Trans.* **1979**, 723–726.

Scheme 1



$[\{\text{Cu}^{\text{II}}_2(\text{PD}'\text{O}^-)(\text{OH}^-)\}_2](\text{ClO}_4)_4$  (**8**). **2** (48 mg, 0.05 mmol) was dissolved in 8 mL of  $\text{O}_2$ -free propionitrile (under Ar), giving a bright yellow solution. This was cooled to  $-80^\circ\text{C}$  in a dry ice/acetone bath, and  $\text{O}_2$  was slowly (to minimize warming) bubbled through the reaction solution ( $\sim 1$  min) until full formation of **1**. Any  $\text{O}_2$  remaining was removed by argon purging. The resulting solution was then allowed to decay by warming to ambient temperature. A reddish-brown solution was obtained after 2 h. Diethyl ether (100 mL) was added to precipitate the resulting copper complexes. Under argon, the resulting reddish powder was redissolved with 5 mL  $\text{CH}_3\text{CN}$ ; a green crystalline solid (11 mg, 25%) suitable for X-ray crystallographic structural determination was obtained after 2 weeks by slow diffusion of diethyl ether into this solution at  $-20^\circ\text{C}$ . Anal. Calcd for  $(\text{C}_{68}\text{H}_{72}\text{Cl}_4\text{Cu}_4\text{N}_{12}\text{O}_{20})$ : C, 46.06; H, 4.09; N, 9.48. Found: C, 45.73; H, 3.89; N, 9.26; UV-vis (MeCN,  $\lambda_{\text{max}}$ , nm): 445 (sh,  $\epsilon = 240 \text{ M}^{-1} \text{ cm}^{-1}$ ), 803 (br,  $\epsilon = 320 \text{ M}^{-1} \text{ cm}^{-1}$ ); Magnetic Moment:  $1.4 \pm 0.1 \mu_{\text{B}}$  per tetranuclear complex (as determined by the Evans NMR method in  $\text{CD}_3\text{CN}$ ).<sup>34</sup>

## Results and Discussion

**Generation of 1.** The previously studied hydroperoxide bridged dinuclear copper(II) species **1A** could be prepared by three different methods (Scheme 1): (a) Direct oxygenation from the phenol-containing dinuclear Cu(I) complex  $[\text{Cu}_2(\text{XYL}-\text{OH})(\text{L})_2]^{2+}$  (L, external ligand, for instance, acetonitrile) at  $-80^\circ\text{C}$ , (b) protonation of the dinuclear peroxide complex  $[\text{Cu}_2^{\text{II}}(\text{XYL}-\text{O}^-)(\text{O}_2^{2-})]^{2+}$ ,<sup>14</sup> or (c)  $\text{H}_2\text{O}_2$  reaction (at  $\sim -80^\circ\text{C}$ ) with the  $\mu$ -phenoxo- $\mu$ -hydroxo dinuclear Cu(II) complex  $[\text{Cu}_2^{\text{II}}(\text{XYL}-\text{O}^-)(-\text{OH})]^{2+}$  with ligand displacement/substitution.

In the system presently under discussion, **1** could *only* be generated via route (a). Reacting the dicopper(I) complex **2** with molecular  $\text{O}_2$  at  $-80^\circ\text{C}$  in propionitrile gives **1**, which

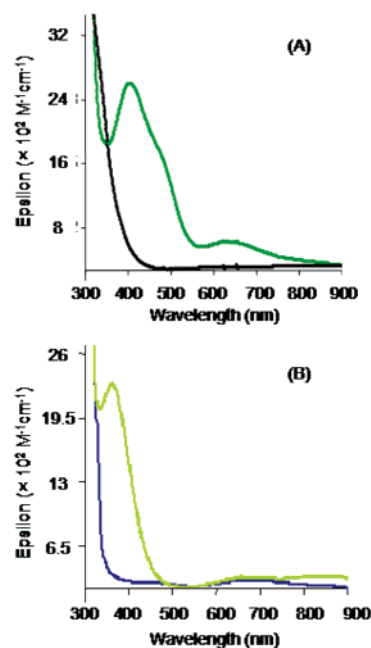
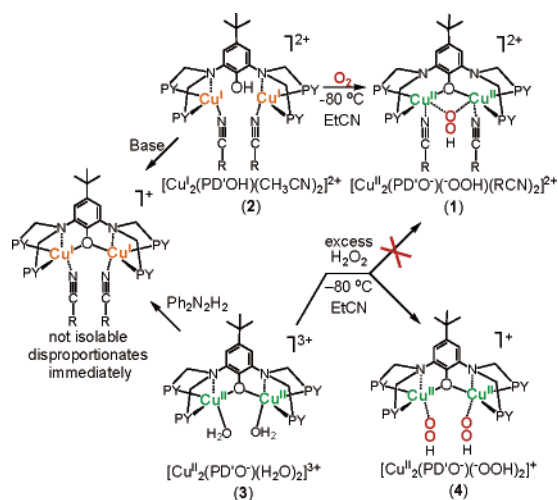


**Figure 1.** (A) UV-vis absorption of  $[\text{Cu}_2(\text{PD}'\text{OH})(\text{MeCN})_2]^{2+}$  (**2**) (black) and  $[\text{Cu}_2^{\text{II}}(\text{PD}'\text{O}^-)(-\text{O}_2\text{H})(\text{EtCN})_2]^{2+}$  (**1**) (green,  $\lambda_{\text{max}} = 407$  nm) at  $-80^\circ\text{C}$  in EtCN. (B) UV-vis absorption of  $[\text{Cu}_2^{\text{II}}(\text{PD}'\text{O}^-)(\text{H}_2\text{O})_2]^{3+}$  (**3**) (blue) and  $[\text{Cu}_2^{\text{II}}(\text{PD}'\text{O}^-)(-\text{O}_2\text{H})_2]^{3+}$  (**4**) (light green,  $\lambda_{\text{max}} = 362$  nm) at  $-80^\circ\text{C}$  in EtCN.

possesses a UV-vis spectrum with absorption maxima at 407 ( $\epsilon = 2700 \text{ M}^{-1} \text{ cm}^{-1}$ ), 488 (sh,  $\epsilon = 1600 \text{ M}^{-1} \text{ cm}^{-1}$ ), and 622 nm ( $\epsilon = 600 \text{ M}^{-1} \text{ cm}^{-1}$ ) (Figure 1A) and an O–O stretching vibration at  $870 \text{ cm}^{-1}$  ( $\Delta(^{18}\text{O}_2) = -50 \text{ cm}^{-1}$ ) in its resonance Raman (rR) spectrum.<sup>30</sup> Both data compare closely with structurally related  $\mu$ -phenoxo- $\mu$ -1,1-hydroperoxo complexes  $[\text{Cu}_2^{\text{II}}(\text{XYL}-\text{O}^-)(-\text{O}_2\text{H})]^{2+}$  (**1A**, Chart 1) and  $[\text{Cu}_2^{\text{II}}(\text{UN}-\text{O}^-)(-\text{O}_2\text{H})]^{2+}$  (**1B**, Chart 1,  $\nu_{\text{O}-\text{O}} = 892 \text{ cm}^{-1}$  ( $\Delta(^{18}\text{O}_2) = -52 \text{ cm}^{-1}$ ).<sup>14,16,17</sup> Complexes **1A** and **1B** possess  $\text{Cu}\cdots\text{Cu}$  distances of  $\sim 3 \text{ \AA}$ ,<sup>14,16</sup> but as we have explained,<sup>30</sup> this normally cannot be fulfilled within the  $\text{PD}'\text{O}^-$  ligand framework. If copper(II) ions sit in the coordination pocket and interact with all three nitrogens of the dipicolylamine (PY1) unit, plus the phenolate oxygen, the  $\text{Cu}\cdots\text{Cu}$  distance would be  $>3.7 \text{ \AA}$ , which is far too long to maintain a  $\mu$ -phenoxide and  $\mu$ -1,1-hydroperoxide coordination. We thus hypothesized that **1** possesses a coordination where the alkylamino N atoms are not copper-bound and nitrile molecules from the solvent instead coordinate with the copper ions (Scheme 2). Supporting this hypothesis: (i) The metal–metal distance in related binucleating ligand frameworks can decrease dramatically through weakening or loss of the bridgehead  $\text{N}_{\text{alkylamino}}$  coordination.<sup>35</sup> (ii)  $\text{Cu}^{\text{II}}$ –nitrile coordination is preceded in a complex closely related to **1**.<sup>15</sup> (iii) Formation of **1** occurs only in nitrile solvents, unlike other systems, suggesting RCN involvement in the chemistry and stabilization **1**. Thus, when **2** reacts with  $\text{O}_2$ , each Cu ion releases the weakly coordinated  $\text{N}_{\text{alkylamino}}$  atom and the hydroperoxide formed (i.e., **1**) is a nitrile solvent-coordinated (and stabilized) species (Scheme 2).

(35) Bauer-Siebenlist, B.; Meyer, F.; Farkas, E.; Vidovic, D.; Cuesta-Seijo, J. A.; Herbst-Irmer, R.; Pritzkow, H. *Inorg. Chem.* **2004**, *43*, 4189–4202.

Scheme 2



As mentioned, reacting  $\text{H}_2\text{O}_2$  with a ligand–copper(II) complex in the presence of base has also proved to be effective in terms of preparation of a variety of  $\text{Cu}_n\text{—OOH}$  species ( $n = 1^{20-25}$  or  $2^{14,18,19,36}$ ). To determine if **1** could be generated by an analogous procedure, **3**<sup>32</sup> was employed in a reaction with excess  $\text{H}_2\text{O}_2$  in the presence of triethylamine. In propionitrile at  $-80^\circ\text{C}$ , a new yellowish-green species formed, possessing a LMCT absorption maxima at 362 nm ( $\epsilon = 2200 \text{ M}^{-1} \text{ cm}^{-1}$ ) and weak absorptions at 690 (150) and 850 nm (190) (Figure 1B). These features do not match those determined for  $\mu$ -1,1-hydroperoxo species **1**; however, by analogy to UV–vis spectra established for terminally bound  $\text{Cu}^{\text{II}}\text{—OOH}$  moieties,<sup>20–25</sup> the formation of a bis copper–hydroperoxo complex **4** is suggested (Scheme 2) (also see further discussion below).

To provide further evidence for the  $(\text{Cu}^{\text{II}}\text{—OOH})_2$  moiety proposed, **4** was generated in a DMF/toluene (1:1) mixed solvent and investigated by EPR spectroscopy. The bridged hydroperoxide complex **1** is EPR silent, consistent with its possessing doubly bridged (phenoxide and hydroperoxide) antiferromagnetically coupled copper(II) ions and in line with the known properties of **1A** and **1B**. By contrast, the EPR spectrum of **4** exhibits a distinctive copper ‘dimer’ EPR spectrum, with multiple-line splitting near  $g \approx 2$  (Figure 2), suggesting that it possesses a triplet ground state, i.e., with two ferromagnetically coupled copper centers.<sup>37</sup> This type of dimer EPR spectra is well known, studied both theoretically and experimentally for a variety of dinuclear copper complexes.<sup>38–41</sup> In fact, the EPR spectrum of **4** is reminiscent of that observed for **3**; this exhibits a well-resolved seven-line EPR spectrum and has been fully analyzed in terms of

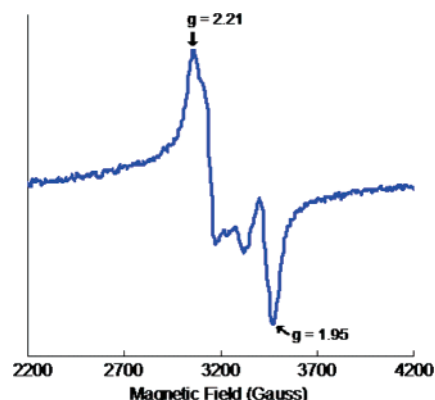


**Figure 2.** EPR spectrum of  $[\text{Cu}^{\text{II}}_2(\text{PD}'\text{O}^-)(\text{O}_2\text{H})_2]^+$  (**4**) in DMF/toluene (1:1). Experimental conditions: temperature, 14 K; microwave frequency, 9.473 GHz; microwave power, 0.201 mW; 100 kHz field modulation amplitude, 0.25 mT (10 G = 1 mT); time constant, 10.24 ms; scan time, 20.97 s.

it possessing ferromagnetically coupled copper(II) centers.<sup>42</sup> The structure of the singly phenolate-bridged complex **3** (Scheme 2) shows that  $\text{Cu}\cdots\text{Cu} = 4.05 \text{ \AA}$ , which is also indicated by the splitting of the two ‘outer’ more intense frozen solution EPR absorptions.<sup>32,42</sup> This splitting for **4** (Figure 2) closely matches that seen for **3**. Thus, the structures of **3** and **4** must be very similar, and this supports the bis  $(\text{Cu}^{\text{II}}\text{—O}_2\text{H})_2$  formulation for **4** (Scheme 2), where hydroperoxide ligands have replaced coordinated  $\text{H}_2\text{O}$  molecules in **3**.

The inability to generate the  $\text{Cu}_2\text{—OOH}$  species **1** following addition of  $\text{H}_2\text{O}_2$  to complex **3** is not easy to fully explain, but the observation does in fact reflect the known structural properties and nature of the  $\text{PD}'\text{O}^-$  ligand. In the direct oxygenation reaction of **2** to yield **1**, thermodynamically favored copper(I) oxygenation by molecular  $\text{O}_2$  acts as the reaction driving force and only 1 mol equiv of  $\text{O}_2$  will add per dicopper(I) moiety, (leading to 1 mol equiv of hydroperoxide per dicopper(II) group). By contrast, during the addition of the  $\text{H}_2\text{O}_2$  to **3**, a redox reaction is not involved. To form the bridging hydroperoxide complex **1**, the  $\text{Cu}\text{—N}_{\text{bridgehead}}$  bond in the thermodynamically stabilized complex **3** would have to be replaced by  $\text{Cu}\text{—N}_{\text{nitrile}}$  bonds to allow the two copper ions to move toward each other ( $\sim 1 \text{ \AA}$ ) enabling the formation of the bridged  $\text{—OOH}$  group. Instead, two  $\text{OOH}$  ligands replace two water molecules in **3**, with little structural change, forming **4**.

One method by which we had hoped to also generate **1** was to synthesize a phenoxide-bridged dicopper(I) complex with  $\text{PD}'\text{O}^-$ . Oxygenation of this copper(I) complex would give a peroxide species, which absorbs a proton to yield **1**, analogous to one method employed to give **1A** (Scheme 1).<sup>14</sup> Phenolate-bridged dinuclear copper(I) complexes are well known in the literature.<sup>43–46</sup> However, addition of 1 equiv

(36) Cruse, R. W.; Kaderli, S.; Meyer, C. J.; Zuberhuhler, A. D.; Karlin, K. D. *J. Am. Chem. Soc.* **1988**, *110*, 5020–5024.

(37) An EPR absorption expected for a ‘dimer’ copper compound EPR spectrum, at  $g \approx 4$ , corresponding to the expected  $M_s = 2$  transition, was not resolvable with the relatively poor signal-to-noise ratio we could obtain.

(38) Bencini, A.; Gatteschi, D.; Zanchini, C.; Haasnoot, J. G.; Prins, R.; Reedijk, J. *Inorg. Chem.* **1985**, *24*, 2812–2815.

(39) Smith, T. D.; Pilbrow, J. R. *Coord. Chem. Rev.* **1974**, *13*, 173–278.

(40) Oyoung, C. L.; Dewan, J. C.; Lillenthal, H. R.; Lippard, S. J. *J. Am. Chem. Soc.* **1978**, *100*, 7291–7300.

(41) Berends, H. P.; Stephan, D. W. *Inorg. Chem.* **1987**, *26*, 749–754.

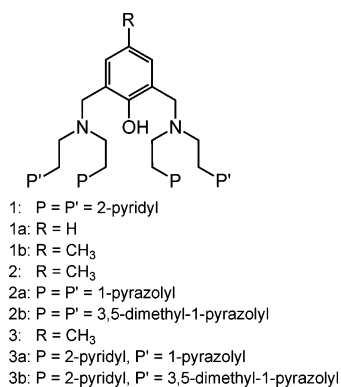
(42) Li, L.; Murthy, N. N.; Telser, J.; Zakharov, L. N.; Yap, G. P.; Rheingold, A. L.; Karlin, K. D.; Rokita, S. E. *Inorg. Chem.* **2006**, *45*, 7144–7159.

(43) Sorrell, T. N.; Borovik, A. S. *J. Chem. Soc. Chem. Comm.* **1984**, 1489–1490.

(44) Sorrell, T. N.; Shen, C. C.; Oconnor, C. J. *Inorg. Chem.* **1987**, *26*, 1755–1758.

(45) Gagne, R. R.; Kreh, R. P.; Dodge, J. A. *J. Am. Chem. Soc.* **1979**, *101*, 6917–6927.

Chart 2



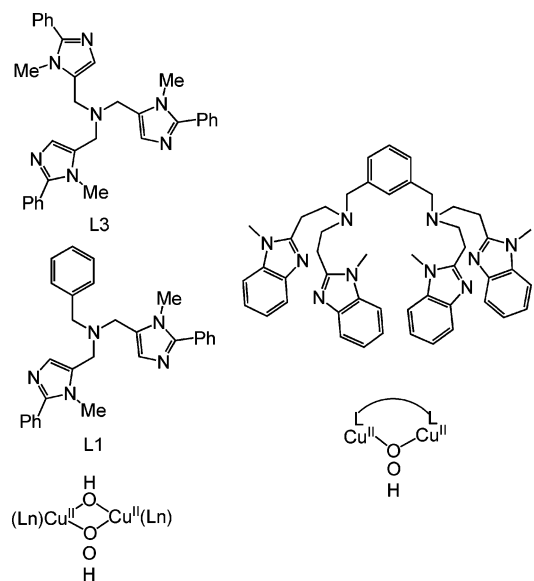
of base to **2** or reduction of **3** by diphenylhydrazine (as a two-electron two-proton source) led to the formation of an orange-colored solution, which immediately underwent disproportionation. We propose that distortion caused by the rigid PD'O<sup>-</sup> ligand destabilizes the resulting dicopper(I) complex (Scheme 2). Similar disproportionation reactions were observed by Sorrell and co-workers.<sup>47</sup>

**UV–Vis Absorption of 1 and 4.** Table S1 (Supporting Information)<sup>48</sup> contains a large listing of known hydroperoxo–copper(II) complexes, mononuclear and binuclear, along with UV–vis and vibrational (e.g.,  $\nu(\text{O}–\text{O})$  values from rR) spectroscopic data and literature references. The UV absorption of complex **1** closely mimics its  $\mu$ -1,1-hydroperoxo-dicopper(II) structural analogues **1A** and **1B** (Table S1).<sup>14,16,48</sup> It possesses a strong absorption with  $\lambda_{\text{max}} = 407$  nm having a shoulder at 489 nm and a weak band at 622 nm (Figure 1A and Table S1). By analogy to **1A** and **1B**, we assign the 407 nm band as a hydroperoxo-to-Cu(II) LMCT transition. The absorption is of lower intensity than for the corresponding peaks in **1A** and **1B**, suggesting a less covalent overlap of the <sup>-</sup>OOH and copper(II) LUMO orbitals, likely due to geometric constraints and the lack of hydrogen bonding (no H-bonding solvent present) for this system.<sup>30</sup>

Sorrell and co-workers synthesized a series of analogues of **1A** and **1B** (Chart 1) in which pyrazolyl donors are present in place of two or four of the pyridyl ligands (Chart 2).<sup>47</sup> In fact, these complexes all exhibit absorption spectra similar to those of **1A** and **1B**. Gaussian fitting of the absorption spectra of  $[\text{Cu}^{\text{II}}_2(\text{UN}–\text{O}^-)(-\text{O}_2\text{H})]^{2+}$  and Sorrell's analogous complex  $[\text{Cu}^{\text{II}}_2(\text{L2b})(-\text{OOH})]^{2+}$  showed that at least three electronic transitions lie under the 400 nm absorption envelope, which may be assigned as phenolate-to-copper CT and/or additional hydroperoxo-to-copper(II) CT transitions.<sup>17</sup> Similar phenolate-related electronic transitions may also contribute to the 407 nm absorption in **1**. We attribute the 622 nm band in **1** as a ligand-field transition; this broad absorption feature is typical for d–d transitions within a square pyramidal copper(II) complex ligand environment.

The two  $\mu$ -hydroxo- $\mu$ -hydroperoxo dicopper(II) complexes recently described by Suzuki and co-workers (Chart 3,

Chart 3



Ligand L1 and L3 have intense LMCT bands at 356 (6300) and 341 nm (7000) respectively,<sup>18</sup> similar to the intense UV–vis band at 342 nm (12 000) of the benzimidazole ligand-containing  $\text{Cu}_2\text{–OOH}$  species obtained by Casella and co-workers (that which was found to be able to hydroxylate the xylyl ring, Chart 3).<sup>19</sup> Relative to these structurally similar  $\mu$ -hydroperoxo-dicopper(II) complexes, **1** possesses a very red-shifted (to the 407 nm envelope, Table S1) hydroperoxo-related LMCT band; no relevant absorption occurs at lower than 400 nm. This lower-energy band must relate to the difference in overall molecular electronic structure; for one thing, **1** possesses a  $\mu$ -phenolate bridging donor ligand, whereas the others do not (Chart 3).

The UV absorption maxima at 362 (2200) nm for **4** is within the typical absorption range of 350–380 nm for LMCT transition in a variety of mononuclear  $\text{Cu}–\text{OOH}$  species (Table S1), with one exception,  $[\text{Cu}^{\text{II}}(\text{HB}(3\text{'Bu}-5\text{'Prpz})_3(-\text{OOH}))]^+$ , with LMCT band at 600 nm (1540).<sup>29</sup> These UV–vis characteristics further support the formulation of **4** and structure described above, possessing (two) terminally bound  $\text{Cu}^{\text{II}}(-\text{OOH})$  moieties, in a dicopper(II) triplet ground-state complex with a structure similar to **3**.

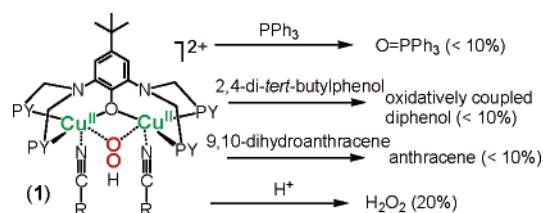
**rR Spectroscopy of 1.** As we reported in our preliminary communication, the rR spectrum of **1** reveals an O–O stretching vibration at 870  $\text{cm}^{-1}$ , which downshifts to 820  $\text{cm}^{-1}$  upon <sup>18</sup>O-labeling. If  $\text{B}(\text{C}_6\text{F}_5)_4^-$  was used as the counteranion, the O–O stretching vibration appears at 855  $\text{cm}^{-1}$  with  $-45$  to  $-50$   $\text{cm}^{-1}$  <sup>18</sup>O isotopic shift.<sup>30</sup> These data compare closely to that of **1B** ( $\nu_{\text{O}–\text{O}} = 892$   $\text{cm}^{-1}$ ) ( $\Delta(^{18}\text{O}_2) = -52$   $\text{cm}^{-1}$ ) (Table S1).<sup>17</sup> The O–O stretches in **1** are also comparable with the two  $\mu$ -hydroxo- $\mu$ -hydroperoxo dicopper(II) species synthesized by Suzuki and co-workers ( $\nu_{\text{O}–\text{O}} = 868$   $\text{cm}^{-1}$  ( $-45$   $\text{cm}^{-1}$ ) or 883  $\text{cm}^{-1}$  ( $-50$   $\text{cm}^{-1}$ ) Chart 3).<sup>18</sup> Although no  $\nu_{\text{Cu}–\text{O}}$  stretch is observed above the signal-to-noise ratio in this photosensitive compound **1**, both UV absorption and rR data are thus consistent with its proposed

(46) Karlin, K. D.; Cruse, R. W.; Gultneh, Y.; Farooq, A.; Hayes, J. C.; Zubieta, J. *J. Am. Chem. Soc.* **1987**, *109*, 2668–2679.

(47) Sorrell, T. N.; Vankai, V. A. *Inorg. Chem.* **1990**, *29*, 1687–1692.

(48) See Supporting Information.

Scheme 3



structure as being the same as **1A** and **1B** with one  $\mu$ -phenoxo bridging ligand plus a  $\mu$ -1,1-OOH donor (Table S1).<sup>48</sup>

For end-on peroxo dicopper(II) species,  $\nu_{(O-O)}$  falls in the 820–840  $\text{cm}^{-1}$  region, while for side-on peroxo  $\mu$ - $\eta^2$ : $\eta^2$ -dicopper(II) species, they are usually observed in the 730–760  $\text{cm}^{-1}$  range due to an additional Cu–O bond interaction and O–O bond weakening.<sup>8,49</sup> Thus, the O–O stretches for these bridging  $\text{Cu}_2$ –OOH species (**1**, **1A**, or **1B**, for instance) are higher than those observed in the nonprotonated copper–peroxide complexes, suggesting stronger O–O bonds in  $\text{Cu}_2$ –OOH species, as previously explained.<sup>17,29</sup>

Mononuclear Cu–OOH species typically have a  $\nu_{(O-O)}$  value between 830  $\text{cm}^{-1}$  and 860  $\text{cm}^{-1}$ , thus the 870  $\text{cm}^{-1}$  vibration in  $\mu$ -hydroperoxide **1** is greater. This in fact may not indicate a stronger O–O bond, as reflected by the reactivity studies of compound **1** (see discussions below). Chen and Solomon<sup>29</sup> compared the O–O bond strength of the mononuclear  $[\text{Cu}^{\text{II}}(\text{HB}(3\text{-}^t\text{Bu}-5\text{-}^i\text{Prpz})_3)(\text{OOH})]^+$  and dinuclear **1B** species, determining that the O–O bond force constants for these two hydroperoxo complexes are nearly identical. The higher frequency  $\nu_{(O-O)}$  for the  $\text{Cu}_2$ –OOH relative to that of the Cu–OOH moiety is due to an increased mechanical coupling between the Cu–O and O–O vibrations.<sup>29</sup> It may be of future interest to carry out a rR study on these two closely related complexes, **1** and **4**, to shed further light on the nature of these  $\text{Cu}_n$ –OOH species.

**Exogenous Substrate Reactivity of 1.** We have previously observed that dinuclear  $\mu$ -1,1-copper(II) hydroperoxide species are reasonable oxidants, especially compared to their nonprotonated peroxo counterparts. For instance, **1A** stoichiometrically oxidizes  $\text{PPh}_3$  to  $\text{O}=\text{PPh}_3$  while the addition of  $\text{PPh}_3$  to the corresponding peroxide complexes  $[\text{Cu}^{\text{II}}_2(\text{XYL}-\text{O}^-)(\text{O}_2^{2-})]^+$  species releases molecular  $\text{O}_2$  and yields a corresponding dicopper(I)( $\text{PPh}_3$ )<sub>2</sub> adduct.<sup>14</sup> By contrast, addition of 1–2 equiv of  $\text{PPh}_3$  to **1** EtCN solution at  $-80^\circ\text{C}$  followed by warming to room temperature led to the formation of a reddish-brown solution, but GC analysis indicated that only  $\sim 10\%$  (based on **1**) of the added  $\text{PPh}_3$  was converted to  $\text{O}=\text{PPh}_3$ . Also, very low yields of typical oxidation products of 2,4-di-*tert*-butylphenol or 9,10-dihydroanthracene were observed when these were employed as substrates (Scheme 3). Furthermore, addition of acid to **1** might be expected to liberate near-stoichiometric yields of hydrogen peroxide, as were found with the  $\text{XYL}-\text{O}^-$  and  $\text{UN}-\text{O}^-$  systems **1A** and **1B** (Chart 1).<sup>14,16</sup> Protonation of **1**

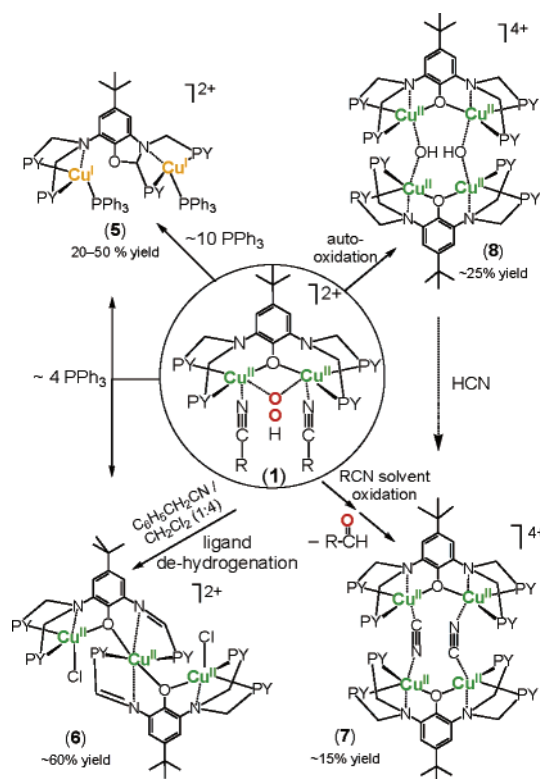


**Figure 3.** Summary of ligand-based thermal transformation reactions undergone by hydroperoxodicopper(II) complex  $[\text{Cu}^{\text{II}}_2(\text{PD}'\text{O}^-)(\text{O}_2\text{H})\text{EtCN}]_2^{2+}$  (**1**).

with  $\text{HPF}_6/\text{Et}_2\text{O}$  at  $-80^\circ\text{C}$  immediately changed the color of the solution from green to blue; however, workup (Experimental Section) afforded only an  $\sim 20\%$  yield of hydrogen peroxide (Scheme 3).

As will be seen in the discussions below, several other oxidative reactions occur on the  $\text{PD}'\text{O}^-$  ligand itself, and these intramolecular processes most likely very favorably compete with the reactions of exogenous substrates described by Scheme 3.

**Decay Reactions of 1.** In fact, hydroperoxo dicopper(II) complex **1** undergoes a variety of interesting  $\text{PD}'\text{O}^-$  ligand-based oxidative transformations. We have been able to isolate and structurally characterize three new products, accounting for the several competing processes which seem to occur. Figure 3 provides an overview/summary.

**Decay of 1 in the Presence of Excess  $\text{PPh}_3$ .** When 4 equiv of  $\text{PPh}_3$  were added to **1** in EtCN at  $-80^\circ\text{C}$  and the reaction mixture stirred, the solution gradually lost its distinctive green color, and over a 3 h period, a pink-colored species with a new LMCT maxima at 540 nm gradually developed (pink spectrum, Figure 4). Warming this solution to room temperature produced a reddish-brown species with a UV absorption at  $\lambda_{\text{max}} = 460$  nm (not shown in Figure 4). From this solution (which is a mixture, see further discussion below), crystallization afforded an orange material. The UV–vis absorption spectrum of isolated material, compound **5**, reveals  $\lambda_{\text{max}} = 335, 400$  nm (sh) (see X-ray structure, below), without any 460 nm absorption present, indicating that it is not the major product under the reaction conditions employed. This supposition is also consistent with the

(49) Komiyama, K.; Furutachi, H.; Nagatomo, S.; Hashimoto, A.; Hayashi, H.; Fujinami, S.; Suzuki, M.; Kitagawa, T. *Bull. Chem. Soc. Jpn.* **2004**, *77*, 59–72.

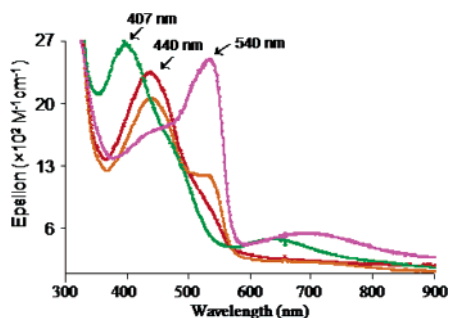


**Figure 4.** UV-vis absorption of  $[\text{Cu}_2(\text{PD}'\text{O}^-)(\text{RCN})_2]^{2+}$  (**1**) ( $\lambda_{\text{max}} = 407$  nm) decomposition at  $-80$  °C in EtCN in the presence of a 10-fold excess of  $\text{PPh}_3$ . A pink solution ( $\lambda_{\text{max}} = 540$  nm) gradually forms in the next several hours following  $\text{PPh}_3$  addition, while a red solution ( $\lambda_{\text{max}} = 440$  nm) gradually develops in the next few weeks: 10 days, orange line; 18 days, red line. Warming this solution up to ambient temperature leads to the formation of the dicopper(I) complex  $[\text{Cu}_2(\text{L}')(\text{PPh}_3)_2](\text{ClO}_4)_2$  (**5**) ( $\lambda_{\text{max}} = 335$  nm, 400 nm (sh)). See text.

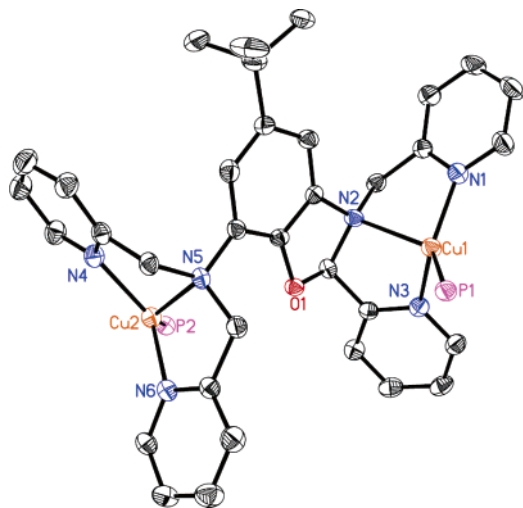


**Figure 5.** X-ray structure of the cross-linked ligand containing dinuclear copper(I) complex  $[\text{Cu}_2(\text{L}')(\text{PPh}_3)_2]^{2+}$  (**5**,  $\text{L}'$  cross-linked ligand); the  $\text{PPh}_3$  phenyl groups have been omitted for clarity; a fully labeled drawing is available.<sup>48</sup>  $\text{Cu}-\text{N}_{\text{py}} = 2.02\text{--}2.27$  Å;  $\text{Cu}-\text{P} = 2.18$  Å;  $\text{Cu}\cdots\text{Cu} = 6.84$  Å.

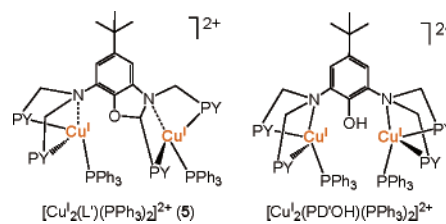
observed  $\sim 20\%$  yield. The presence of competing reaction pathways (Figure 3) seems likely as we also observe that no product **5** is isolated if only 1 equiv of  $\text{PPh}_3$  is used in the reaction with **1**. However, with 10 equiv of  $\text{PPh}_3$  added to **1** at  $-80$  °C followed by thermal decay, a 51% yield of **5** is obtained (Figure 3, Experimental Section).

The structure of **5** ( $\text{L}'$  cross-linked ligand, Figure 3) is shown in Figure 5; selected bond angles and distances are provided in Table 1).<sup>48</sup> Each copper ion (now reduced to copper(I)) is coordinated by a  $\text{PPh}_3$  molecule. A most interesting feature revealed is the presence of a newly formed ligand heterocyclic five-membered ring, where the phenolate oxygen and the methylene carbon on one of the four ligand arms have been coupled. This is a formally a two-electron oxidative process, in fact reminiscent of what occurs between a tyrosine and histidine in certain heme proteins.<sup>50,51</sup> The  $\text{N}_{\text{amino}}$  and O atoms (of course) remain in the plane of the

**Table 1.** Selected Distances and Angles for  $[\text{Cu}_2(\text{L}')(\text{PPh}_3)_2](\text{ClO}_4)_2$  (**5**)

Bond lengths (Å)		
$\text{Cu}(1)-\text{N}(1)$	2.026(2)	$\text{Cu}(2)-\text{N}(4)$ 2.050(2)
$\text{Cu}(1)-\text{N}(2)$	2.254(2)	$\text{Cu}(2)-\text{N}(5)$ 2.266(2)
$\text{Cu}(1)-\text{N}(3)$	2.057(2)	$\text{Cu}(2)-\text{N}(6)$ 2.062(2)
$\text{Cu}(1)-\text{P}(1)$	2.1797(7)	$\text{Cu}(2)-\text{P}(2)$ 2.1753(7)
$\text{O}(1)-\text{C}(7)$	1.455(3)	
Bond Angles (deg)		
$\text{N}(1)-\text{Cu}(1)-\text{N}(2)$	79.65(8)	$\text{N}(4)-\text{Cu}(2)-\text{N}(5)$ 79.87(8)
$\text{N}(1)-\text{Cu}(1)-\text{N}(3)$	115.87(8)	$\text{N}(4)-\text{Cu}(2)-\text{N}(6)$ 121.96(8)
$\text{N}(1)-\text{Cu}(1)-\text{P}(1)$	130.68(7)	$\text{N}(4)-\text{Cu}(2)-\text{P}(2)$ 117.05(6)
$\text{N}(2)-\text{Cu}(1)-\text{N}(3)$	78.48(8)	$\text{N}(5)-\text{Cu}(2)-\text{N}(6)$ 78.74(8)
$\text{N}(2)-\text{Cu}(1)-\text{P}(1)$	131.55(6)	$\text{N}(5)-\text{Cu}(2)-\text{P}(2)$ 135.71(6)
$\text{N}(3)-\text{Cu}(1)-\text{P}(1)$	108.30(6)	$\text{N}(6)-\text{Cu}(2)-\text{P}(2)$ 115.89(6)
$\text{O}(1)-\text{C}(7)-\text{N}(2)$	103.27(18)	
$\text{N}(2)-\text{C}(7)-\text{C}(8)$	112.6(2)	$\text{C}(18)-\text{O}(1)-\text{C}(7)$ 104.82(18)
$\text{O}(1)-\text{C}(7)-\text{C}(8)$	110.6(2)	
Cu $\cdots$ Cu Distance (Å)		
$\text{Cu}(1)\cdots\text{Cu}(2)$	6.839 Å	

**Chart 4**



original phenol with the C derived from the methylene group is now  $\sim 0.4$  Å out of that plane (Figure 5).

We can compare this structure to the dinuclear Cu(I) complex with the original  $\text{PD}'\text{OH}$  ligand  $[\text{Cu}_2(\text{PD}'\text{OH})(\text{PPh}_3)_2]^{2+}$ .<sup>30</sup> Half of complex **5** with the full PY1 group (left portion, Figure 5) is structurally nearly identical to that observed in  $[\text{Cu}_2(\text{PD}'\text{OH})(\text{PPh}_3)_2]^{2+}$  (Chart 4),<sup>30</sup> while the other half with the newly formed heterocyclic ring, has slightly elongated (0.03–0.05 Å) copper(I)–ligand bond lengths and somewhat modified ( $< 15^\circ$ ) bond angles about the copper ion. The  $\text{Cu}\cdots\text{Cu}$  distance is increased from 6.379 Å in  $[\text{Cu}_2(\text{PD}'\text{OH})(\text{PPh}_3)_2]^{2+}$  to 6.839 Å in **5**.

To further confirm the formation and nature of **5**, 10 equiv of KCN was added to the orange solution developed from the **1** + 10  $\text{PPh}_3$  reaction followed by the warming to remove the copper ion from solution complexes (by cyanide complexation) and isolate the organics (i.e., the ligand(s)) present (Scheme 4).<sup>33</sup> A  $\text{PD}''\text{OH}$  analogue with three rather than four pyridylmethyl arms,  $\text{PD}''\text{OH}$  (Scheme 4), was subsequently isolated ( $\sim 65\%$  yield) and identified. Its formation is consistent with the prior presence of  $\text{L}'$  within the structure of **5**, as  $\text{PD}''\text{OH}$  should readily form from hydrolytic ring opening and elimination (Scheme 4). Thus, the major product produced by excess  $\text{PPh}_3$  reaction with **1** is **5**, produced by reduction and phosphine adduct formation. Separately, as isolated by column chromatography,  $\text{O}=\text{PPh}_3$  was obtained in  $\sim 60\%$  yield (see Experimental Section). We did not investigate the source of the oxygen atom in this product. It may have derived from the  $^-\text{OOH}$  moiety in **1** by oxo-transfer<sup>14–16</sup> or from water/hydroxide present, see discussion below.

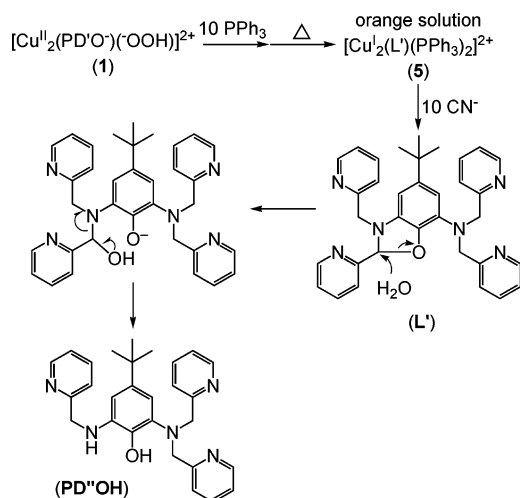
Formation of the C–O bond in the heterocyclic ring in **5** suggests the involvement of ligand  $\text{PD}'\text{O}^-$ -derived phenoxyl

(50) Okeley, N. M.; Van der Donk, W. A. *Chem. Biol.* **2000**, *7*, R159–R171.

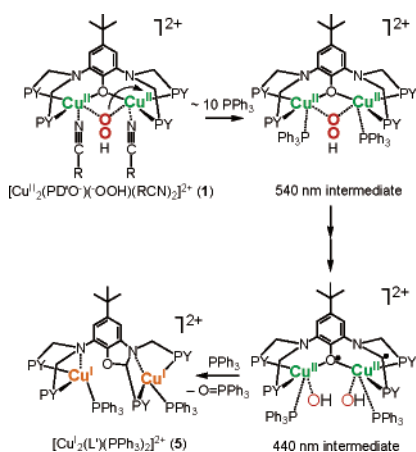
(51) Bravo, J.; Fita, I.; Ferrer, J. C.; Ens, W.; Hillar, A.; Switala, J.; Loewen, P. C. *Protein Sci.* **1997**, *6*, 1016–1023.



## Scheme 4



## Scheme 5



and methylene ligand arm carbon radicals which couple to give the new O–C bond (Scheme 5). Methylene-derived carbon radical formation is a reasonable supposition based on (i) our previously detailed **1**-mediated hydrogen atom abstraction on a  $-\text{CH}_2-$  group alpha to a coordinated nitrile<sup>30</sup> and (ii) the nature of other products formed by thermal decay of **1** (vide infra). We suggest that the added  $\text{PPh}_3$  plays a key role in the corresponding phenoxyl radical generation, facilitating  $\text{Cu}^{\text{II}}$ -to- $\text{Cu}^{\text{I}}$ -( $\text{PPh}_3$ ) with  $\text{ArO}$ -to- $\text{ArO}^\bullet$  conversions; this would be strongly favored by copper(I) stabilization via  $\text{PPh}_3$  coordination.

To obtain further insights, we followed the compound **1** decay process with 10-fold excess of  $\text{PPh}_3$  by UV–vis spectroscopy at  $-80^\circ\text{C}$  (Figure 4). As mentioned before, initially a pink solution developed of compound **1**, yielding a pink species with  $\lambda_{\text{max}} = 540 \text{ nm}$  (Figure 4). We suggest that this might indicate substitution of the coordinated nitrile ligands by  $\text{PPh}_3$  within the hydroperoxide complex (Scheme 5); although  $\text{PPh}_3$  favors copper(I) ligation, it does bind  $\text{Cu}(\text{II})$  ions<sup>52–54</sup> and the excess (10-fold)  $\text{PPh}_3$  would drive the

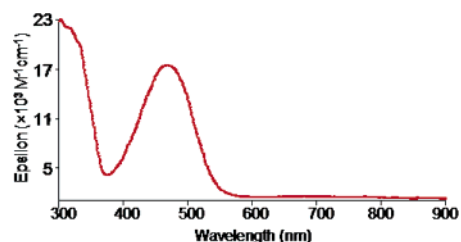
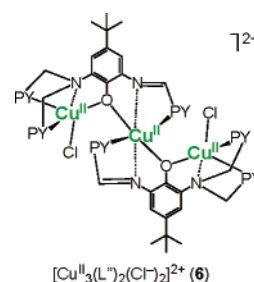


**Figure 6.** UV–vis absorption of red species ( $\lambda_{\text{max}} = 460 \text{ nm}$ ) produced by the  $[\text{Cu}^{\text{II}}_2(\text{PD}'\text{O}^-)(-\text{O}_2\text{H})(\text{RCN})_2]^{2+}$  (**1**) thermal decay reaction at ambient temperature in MeCN.

## Chart 5



reaction. This species may then slowly (over days at  $-80^\circ\text{C}$ , Figure 4) undergo O–O bond cleavage to yield a dicopper(II) coordinated phenoxyl radical red species with  $\lambda_{\text{max}} = 440 \text{ nm}$  (Scheme 5); we suggest this possibility since Michel and co-workers<sup>55</sup> recently described a dicopper(II) phenoxyl radical complex with dinucleating ligand very similar to  $\text{PD}'\text{O}^-$  (with quartet ground state), in fact possessing a 440 nm absorption. Our red species is EPR silent, suggesting that the subsequently formed carbon radical (or copper-bound hydroxy radical as a precursor) might be spin-coupled with this phenoxyl radical. Warming would then lead to heterocyclic ring formation via C–O bond coupling;  $\text{Cu}(\text{II}) \rightarrow \text{Cu}(\text{I})$  reduction accompanied by phosphine oxide formation could lead to the observed final product **5**. Clearly, much of the discussion just above is speculative, but we wish to comment on the possible nature of the observed 540 and 440 nm low-temperature stabilized species; clearly, more research would be required to better understand how **5** forms.

**Decay of 1 in the Absence of  $\text{PPh}_3$ .** As implied by the discussions above, without any added triphenylphosphine to **1**, or even with up to  $\sim 4$  equiv of  $\text{PPh}_3$ , a reddish brown species with visible absorption at 460 nm (now shown here, Figure 6) appears. In fact, the species with this feature, identified as a trinuclear complex **6** (Chart 5), seems to be the primary thermal transformation product as it can be isolated in 56% yield from a reaction in a  $\text{PhCH}_2\text{CN}/\text{CH}_2\text{Cl}_2$  (1:4) solvent mixture (see Experimental Section). In forming, **1** has undergone multiple-step (oxidative) transformations as revealed by its X-ray structure, (Chart 5, Figure 7, Table 2).<sup>48</sup>

An X-ray structure of **6** shows it to be constructed of a dimer of an oxidatively modified  $\text{PD}'\text{O}^-$  ligand (described further, below) which is connected by coordination to an

(52) Koman, M.; Valigura, D.; Durcanska, E.; Ondrejovic, G. *J. Chem. Soc., Chem. Comm.* **1984**, 381–383.

(53) Koman, M.; Valigura, D.; Ondrejovic, G. *Acta Crystallogr. C* **1988**, *44*, 601–603.

(54) Nyburg, S. C.; Parkins, A. W.; Sidiboumedine, M. *Polyhedron* **1993**, *12*, 1119–1122.

(55) Michel, F.; Torelli, S.; Thomas, F.; Duboc, C.; Philouze, C.; Belle, C.; Hamman, S.; Saint-Aman, E.; Pierre, J. L. *Angew Chem., Int. Ed.* **2005**, *44*, 438–441.

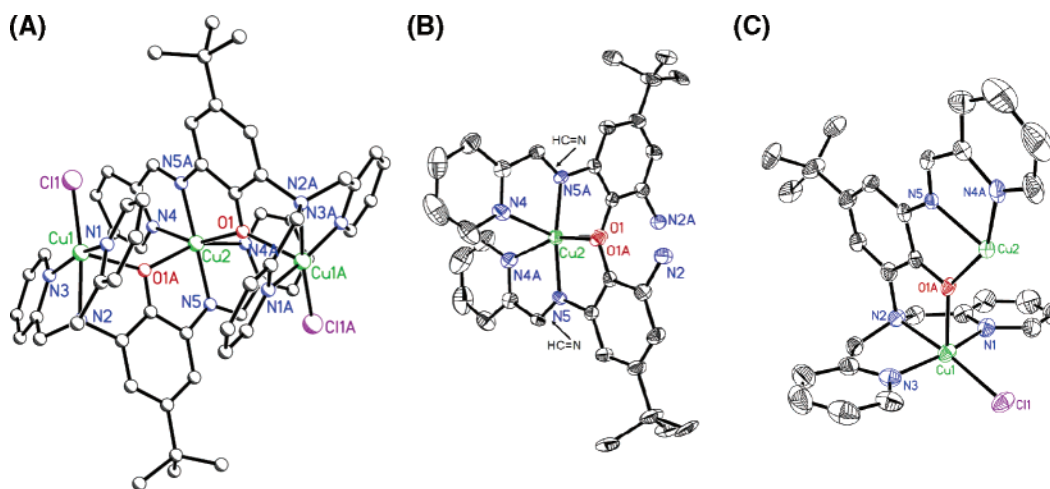


**Figure 7.** X-ray structure of the trinuclear copper complex  $[\text{Cu}_3(\text{L}'')_2(\text{Cl}^-)_2](\text{PF}_6)_2$  (**6**,  $\text{L}''$  Schiff base-containing ligand); (A) Cationic portion of  $[\text{Cu}_3(\text{L}'')_2(\text{Cl}^-)_2]^{2+}$  (**6**); (B) Coordination of just the central hexacoordinated copper(II) ion (Cu2); (C) Structure emphasizing of terminal (end) copper(II) ion centers (here Cu1).  $\text{Cu}-\text{N}_{\text{py}} = 1.99\text{--}2.21$  Å;  $\text{Cu}-\text{Cl} = 2.26$  Å;  $\text{Cu1}\cdots\text{Cu2} = 4.07$  Å; and  $\text{Cu1}\cdots\text{Cu1}' = 6.58$  Å.<sup>48</sup>

**Table 2.** Selected Distances and Angles for  $[\text{Cu}_3(\text{L}'')_2(\text{Cl}^-)_2](\text{PF}_6)_2$  (**6**)

Bond Lengths (Å)			
Cu(1)–O(1)'	2.188(3)	Cu(2)–O(1)'	2.113(3)
Cu(1)–Cl(1)	2.2610(16)	Cu(2)–O(1)	2.113(3)
Cu(1)–N(1)	1.994(5)	Cu(2)–N(4)	2.203(5)
Cu(1)–N(2)	2.079(4)	Cu(2)–N(4)'	2.203(5)
Cu(1)–N(3)	1.988(5)	Cu(2)–N(5)	1.980(4)
O(1)–Cu(1)'	2.188(3)		
C(28)–N(5)'	1.269(6)	N(5)–C(28)'	1.269(6)
Bond Angles (deg)			
O(1)'–Cu(1)–N(1)	94.25(17)	O(1)'–Cu(2)–O(1)	99.6(2)
O(1)'–Cu(1)–N(2)	83.37(15)	O(1)'–Cu(2)–N(4)	91.26(16)
O(1)'–Cu(1)–N(3)	91.11(17)	O(1)'–Cu(2)–N(4)'	155.80(15)
O(1)'–Cu(1)–Cl(1)	104.90(10)	O(1)'–Cu(2)–N(5)	80.30(15)
N(1)–Cu(1)–N(2)	82.6(2)	O(1)'–Cu(2)–N(5)'	94.28(15)
N(1)–Cu(1)–N(3)	163.2(2)	O(1)–Cu(2)–N(4)	155.80(15)
N(1)–Cu(1)–Cl(1)	96.93(15)	O(1)–Cu(2)–N(4)'	91.25(16)
N(2)–Cu(1)–N(3)	82.3(2)	O(1)–Cu(2)–N(5)	94.28(15)
N(2)–Cu(1)–Cl(1)	171.71(14)	O(1)–Cu(2)–N(5)'	80.30(15)
N(3)–Cu(1)–Cl(1)	97.00(16)	N(4)–Cu(2)–N(4)'	87.3(2)
		N(4)–Cu(2)–N(5)	108.92(17)
Cu(2)–O(1)–Cu(1)'	142.13(16)	N(4)–Cu(2)–N(5)'	77.36(18)
		N(4)'–Cu(2)–N(5)	77.36(17)
C(17)–N(5)–Cu(2)	115.1(3)	N(4)'–Cu(2)–N(5)'	108.91(17)
C(28)'–N(5)–C(17)	125.6(4)	N(5)–Cu(2)–N(5)'	171.7(3)
C(28)'–N(5)–Cu(2)	119.0(4)		
N(5)'–C(28)–C(27)	118.8(5)		
Cu $\cdots$ Cu Distance (Å)			
Cu(1) $\cdots$ Cu(2)	4.0680(11)	Cu(1) $\cdots$ Cu(1)'	6.5796(23)

additional central copper(II) ion. The terminal copper ions (Cu1 and Cu1') are ligated by a bridgehead amine and two nitrogen atoms from the pyridyl ligand donors (Figure 7A, C). The endogenous bridging phenolate (O1) and an exogenous chloride complete the pentacoordination. The  $\tau$  value of the copper ions is 0.14, indicating a slightly distorted square pyramidal geometry,<sup>56</sup> with the phenolate oxygen atom (O1, O1') occupying the axial position (Figure 7C). This five-coordinate structural description is comparable to that seen in **3**, where  $\tau = 0.08$ .<sup>42</sup> The presence of  $\text{Cl}^-$  ligands indicates that the  $\text{CH}_2\text{Cl}_2$  solvent has been involved in the (quite obviously) complicated and multistep reaction, as observed in the previously described compound **1A** decom-

position process.<sup>14</sup> The central copper(II) ion is hexacoordinated, with two phenolate oxygens, two bridgehead amino nitrogens and two pyridyl nitrogens as ligands (Figure 7A, B).

The most noteworthy chemical feature revealed by the structure of **6** is the loss of one pyridyl arm from each original PD'OH ligand—a clear sign of the occurrence of ligand oxidation (see further discussion below); the remaining amine nitrogen is double-bonded to its methylene derived carbon atom,  $\text{C}=\text{N} = 1.269(6)$  Å. This double bond enables the pyridyl moiety to be coplanar with the phenolate group; the  $\text{L}''$  ligands (PD'OH derived) in **6** possess an extended conjugated  $\pi$  system. Further structure description is as follows. There are altogether four planes in this molecule: two planes defined by the pyridyl moieties in PY1 groups from different PD'O<sup>-</sup> units and two planes described by the two phenolate rings coupled by the Schiff base-connected pyridyl groups. Except for the carbons in the *tert*-butyl groups, almost all the atoms in this molecule are either on one plane or another.

The presence of Schiff base moieties in **6** explains its dark red color, based on its strong absorption at  $\lambda_{\text{max}} = 460$  nm ( $\epsilon = 18\,000$   $\text{M}^{-1}$   $\text{cm}^{-1}$ ). We attribute this to the CT process from the phenolate oxygen  $p_\pi$  orbital, which is involved with the extended conjugated  $\pi$  system now present in  $\text{L}''$ , to the Cu(II) d “antibonding” orbitals. This assignment is supported by the similar UV absorptions found in other Schiff base–Cu(II) complexes.<sup>57</sup> Such intensely red-colored compounds have also been obtained with other transition metals; their visible absorption maxima are slightly shifted, as expected.<sup>57–60</sup>

When the thermal decay of **1** is allowed to occur in either MeCN or EtCN solvents, we also observed the distinctive

(56) Addison, A. W.; Rao, T. N.; Reedijk, J.; Vanrijn, J.; Verschoor, G. C. *J. Chem. Soc. Dalton Trans.* **1984**, 1349–1356.

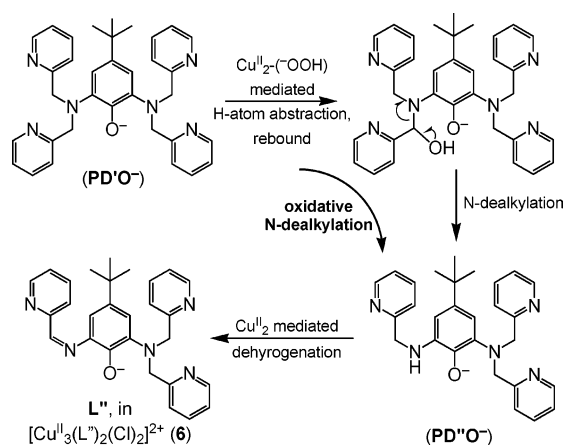
(57) Baran, P.; Boca, R.; Breza, M.; Elias, H.; Fuess, H.; Jorik, V.; Klement, R.; Svoboda, I. *Polyhedron* **2002**, *21*, 1561–1571.

(58) Epstein, D. M.; Choudhary, S.; Churchill, M. R.; Keil, K. M.; Eliseev, A. V.; Morrow, J. R. *Inorg. Chem.* **2001**, *40*, 1591–1596.

(59) Ainscough, E. W.; Brodie, A. M.; Plowman, J. E.; Brown, K. L.; Addison, A. W.; Gainsford, A. R. *Inorg. Chem.* **1980**, *19*, 3655–3663.

(60) Reddig, N.; Triller, M. U.; Pursche, D.; Rompel, A.; Krebs, B. *Z. Anorg. Allg. Chem.* **2002**, *628*, 2458–2462.

Scheme 6



strong 460 nm feature (not shown), suggesting that something akin to the Schiff base-containing ligand trinuclear complex **6** is produced. However, without dichloromethane solvent, there is no chloride source available. The results thus suggest that  $\text{PD}'\text{O}^-$  ligand oxidation is a general reaction during the  $\text{Cu}^{\text{II}}-\text{OOH}$  decomposition, and different side reactions may occur according to the varying solvent/exogenous ligand chemical environments present.

**Oxidative Processes Likely Occurring.** Formation of the Schiff base complex **6** indicates that, during the decay process of **1**, both a ligand oxidative N-dealkylation and subsequent dehydrogenation occur. These may proceed as roughly outlined in Scheme 6. A first step (not shown) is likely to be oxidation of the electron-rich ligand amine atoms to give nitrogen-centered radical cations;  $\text{Cu}(\text{II})$  is known to mediate such reactions.<sup>61–64</sup> Following chemistry gives rise to net  $\text{Cu}^{\text{II}}-\text{OOH}$  hydrogen atom of a  $-\text{CH}_2-$  methylene group to give a carbon-based radical, with ‘rebound’ giving a carbonolamine (hydroxylated ligand). We previously demonstrated an analogous reaction occurred during the nitrile oxidation process induced within **1**; using  $^{18}\text{O}$  and  $^2\text{H}$  labeling of peroxide or substrate nitrile; a small but significant isotope effect was also observed.<sup>30</sup> The ligand  $\text{PD}'\text{O}^-$  methylene groups are susceptible to H-atom abstraction chemistry, as also suggested for the formation of the heterocyclic ring in **5** (vide supra). Subsequent elimination of pyridine-2-carbaldehyde would lead to the overall oxidative N-dealkylation reaction, giving the secondary amine  $\text{PD}''\text{O}^-$  (see also Scheme 4). This, via separate oxidation chemistry, would undergo a ligand dehydrogenation to give  $\text{L}''$ , that seen in complex **6** (Scheme 6). Metal ion complexes containing Ni, Fe, Co, and Cu are known to mediate ligand dehydrogenation reactions, and peroxide complexes are usually involved as the oxidant; a general base also helps deprotonate the substrate (amine  $\text{N}-\text{H}$ ) to initiate or facilitate this reaction.<sup>65–75</sup> In the present system, we however do not really know the oxidant source, as a peroxide group (as in

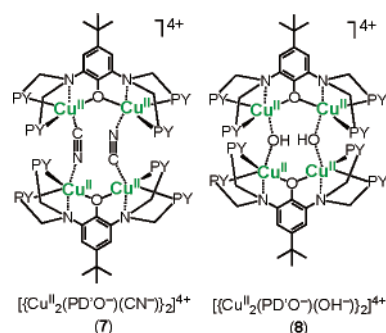
(61) Shearer, J.; Zhang, C. X.; Zakharov, L. N.; Rheingold, A. L.; Karlin, K. D. *J. Am. Chem. Soc.* **2005**, *127*, 5469–5483.

(62) Sumalekshmy, S.; Gopidas, K. R. *Chem. Phys. Lett.* **2005**, *413*, 294–299.

(63) Wang, F.; Sayre, L. M. *Inorg. Chem.* **1989**, *28*, 169–170.

(64) Wang, F.-J.; Sayre, L. M. *J. Am. Chem. Soc.* **1992**, *114*, 248–255.

Chart 6



**1**) as two-electron oxidant has already been ‘used up’ in the first oxidative N-dealkylation reaction. Further, we have little insight into the mechanism by which chloride (which must derive from solvent  $\text{CH}_2\text{Cl}_2$ ) ends up in **6**, although we have previously observed such chloride extraction from dichloromethane with copper complexes under oxidative conditions.<sup>76,77</sup>

**Ligand Methylene vs Exogenous Nitrile Substrate Oxidations.** There are four  $-\text{CH}_2-$  ligand arms and two nitrile molecules which lie in close proximity to the hydroperoxo moiety in **1** (Chart 1). Our reaction chemistry and characterization of products (i.e., **5**, **6**, and **7**) demonstrates that  $\text{C}-\text{H}$  bonds from the four methylene pyridylmethyl arms plus the two  $\alpha\text{-CH}_2$  groups of the coordinated nitriles are all susceptible to oxidation. If one assumes, to a first approximation, that these six positions are equivalent with respect to  $\text{Cu}^{\text{II}}(-\text{OOH})$  group oxidative attack, then the yields of the different products observed might correlate with this chance for attack. In fact, this crude prediction is in reasonable agreement with the actual product yields, which are  $\sim 60\%$  for compound **7**<sup>78</sup> and  $\sim 18\%$  of aldehyde and accompanying tetranuclear cyanide-bridged complex **7** (Chart 6) derived from EtCN oxidation.<sup>30</sup> The highly favored intramolecular oxidation chemistry also explains why external substrates, for instance,  $\text{PPh}_3$  or 2,4-di-*tert*-butylphenol, are not readily oxidized by **1**; they do not compete favorably with the internal intramolecular oxidative processes.

(65) Karlin, K. D.; Gultneh, Y. In *Prog Inorg. Chem.* 1987; Vol. 35; pp 219–327.

(66) Burnett, M. G.; Mckee, V.; Nelson, S. M. *J. Chem. Soc. Chem. Comm.* **1980**, 829–831.

(67) Cabral, J. D.; Cabral, M. F.; Drew, M. G. B.; Esho, F. S.; Nelson, S. M. *J. Chem. Soc. Chem. Comm.* **1982**, 1068–1069.

(68) Basak, A. K.; Martell, A. E. *Inorg. Chem.* **1986**, *25*, 1182–1190.

(69) Basak, A. K.; Martell, A. E. *Inorg. Chem.* **1988**, *27*, 1948–1955.

(70) Raleigh, C. J.; Martell, A. E. *Inorg. Chem.* **1985**, *24*, 142–148.

(71) Raleigh, C. J.; Martell, A. E. *Inorg. Chem.* **1986**, *25*, 1190–1195.

(72) Martell, A. E.; Basak, A. K.; Raleigh, C. J. *Pure Appl. Chem.* **1988**, *60*, 1325–1329.

(73) Hipp, C. J.; Busch, D. H.; Lindoy, L. F. *Inorg. Chem.* **1972**, *11*, 1988–1994.

(74) Dabrowia, Jc; Lovecchi, Fv; Goedken, V. L.; Busch, D. H. *J. Am. Chem. Soc.* **1972**, *94*, 5502–&.

(75) Goedken, V. L.; Busch, D. H. *J. Am. Chem. Soc.* **1972**, *94*, 7355–&.

(76) Lucchese, B. Thesis, Johns Hopkins University, 2003.

(77) Lucchese, B.; Humphreys, K. J.; Lee, D.-H.; Incarvito, C. D.; Sommer, R. D.; Rheingold, A. L.; Karlin, K. D. *Inorg. Chem.* **2004**, *43*, 5987–5998.

(78) Compound **5** cannot be fully isolated from the reaction mixture; consequently, the yield cannot be accurately determined. However, from its distinctive and very high UV absorption, its yield is estimated to be around  $\sim 60\%$ .

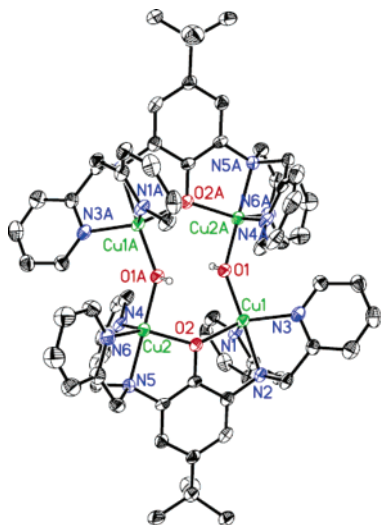


**Figure 8.** X-ray structure of the tetranuclear copper(II) complex  $[\{\text{Cu}^{\text{II}}_2(\text{PD}'\text{O}^-)(\text{OH}^-)\}_2](\text{ClO}_4)_4$  (**8**):  $\text{Cu}-\text{N}_{\text{py}} = 2.03\text{--}2.17$  Å;  $\text{Cu}-\text{O}_{\text{phenolate}} = 2.04$  Å,  $\text{Cu}-\text{O}_{\text{hydroxyl}} = 1.92$  Å; and  $\text{Cu}\cdots\text{Cu} = 3.84_{(\text{intra})}$  and  $3.67_{(\text{inter})}$  Å.<sup>48</sup>

It is noteworthy to look back at past chemistries studied and point out that solvent nitrile oxidation may not be a reaction unique to the  $\text{PD}'\text{O}^-$  system. In nitrile solvents ( $\text{RCN}$ ,  $\text{R} = \text{CH}_3$  or  $\text{CH}_3\text{CH}_2$ ), after the  $\mu$ -hydroperoxide complex **1A** thermally decomposed, the  $\mu$ -hydroxy complex  $[\text{Cu}_2(\text{XYL}-\text{O}^-)(\text{OH}^-)]^{2+}$  formed in high yield.<sup>14</sup> This may have suggested that copper-catalyzed disproportionation of the coordinated (hydro)peroxide took place:  $\mathbf{1A} \rightarrow [\text{Cu}^{\text{II}}_2(\text{XYL}-\text{O}^-)(-\text{OH})]^{2+} + \frac{1}{2}\text{O}_2$ . In fact, no dioxygen was liberated or detected. Thus, we suggest that nitrile oxidation may have occurred in that system but was overlooked. It was also observed that, when **1A** decomposed in  $\text{CH}_2\text{Cl}_2$ , it led to the production of  $[\text{Cu}^{\text{II}}_2(\text{XYL}-\text{O}^-)(\text{Cl}^-)]^{2+}$ .<sup>14,79</sup> As the solvent (e.g.,  $\text{RCN}$  or  $\text{CH}_2\text{Cl}_2$ ) is of course in large excess in these systems, it is reasonable to suppose that its oxidation may be a general occurrence during  $\text{Cu}^{\text{II}}_2-\text{OOH}$  decay.

**Isolation and Characterization of 8.** Formation of Schiff base complex **6** in  $\sim 60\%$  yield along with  $\sim 18\%$  yield of **7** (Chart 6) does not entirely account for an excellent material balance in the thermal decay of **1**. To search for other possible reaction products, solids were precipitated from the reddish-colored  $\text{Cu}^{\text{II}}_2-\text{OOH}$  decomposition products mixture. Recrystallization from  $\text{CH}_3\text{CN}/\text{Et}_2\text{O}$  at  $-20$  °C gave, after 2 weeks, a green crystalline material, tetranuclear complex **8**, in  $\sim 25\%$  yield (X-ray structure: Figure 8, Table 3).<sup>48</sup>

Each molecule of **8** contains two  $\text{PD}'\text{O}^-$  units connected by two bridging hydroxide groups. The cupric ions are all pentacoordinated;  $\tau$  values are found to be 0.8 for Cu1 and 0.61 for Cu2 (on the same  $\text{PD}'\text{O}^-$  binucleating ligand), respectively, meaning that the copper ions have coordination geometry best described as slightly distorted trigonal bipyramidal. This contrasts sharply with the copper environment observed in the dinuclear analogue **3** ( $\tau = 0.08$ ) in which

**Table 3.** Selected Distances and Angles for  $[\{\text{Cu}^{\text{II}}_2(\text{PD}'\text{O}^-)(\text{OH}^-)\}_2](\text{ClO}_4)_4$  (**8**)

Bond Lengths (Å)			
Cu(1)–O(1)	1.915(3)	Cu(2)–O(1)'	1.928(3)
Cu(1)–O(2)	2.043(3)	Cu(2)–O(2)	2.039(3)
Cu(1)–N(1)	2.152(4)	Cu(2)–N(4)	2.170(4)
Cu(1)–N(2)	2.034(4)	Cu(2)–N(5)	2.035(4)
Cu(1)–N(3)	2.077(4)	Cu(2)–N(6)	2.010(4)
		O(1)–Cu(2)#1	1.928(3)
Bond Angles (deg)			
O(1)–Cu(1)–O(2)	95.16(13)	O(1)'–Cu(2)–O(2)	94.77(13)
O(1)–Cu(1)–N(1)	101.28(14)	O(1)'–Cu(2)–N(4)	97.93(15)
O(1)–Cu(1)–N(2)	177.83(15)	O(1)'–Cu(2)–N(5)	178.76(16)
O(1)–Cu(1)–N(3)	101.04(15)	O(1)'–Cu(2)–N(6)	98.35(15)
O(2)–Cu(1)–N(1)	103.83(14)	O(2)–Cu(2)–N(4)	92.61(13)
O(2)–Cu(1)–N(2)	82.69(14)	O(2)–Cu(2)–N(5)	85.32(14)
O(2)–Cu(1)–N(3)	129.81(14)	O(2)–Cu(2)–N(6)	142.16(15)
N(1)–Cu(1)–N(2)	79.01(15)	N(4)–Cu(2)–N(5)	80.83(16)
N(1)–Cu(1)–N(3)	118.67(15)	N(4)–Cu(2)–N(6)	120.22(16)
N(2)–Cu(1)–N(3)	80.63(16)	N(5)–Cu(2)–N(6)	82.30(16)
Cu(1)–O(1)–Cu(2)	145.50(19)		
Cu(1)–O(2)–Cu(2)'	140.64(17)		
Cu $\cdots$ Cu Distance (Å)			
Cu(1) $\cdots$ Cu(2)	3.844	Cu(1) $\cdots$ Cu(2)'	3.671

both copper ions are nearly perfectly square pyramidal.<sup>42</sup> This trigonal bipyramidal copper coordination geometry in **8** enables it to possess a short 3.66 Å intermolecular  $\text{Cu}\cdots\text{Cu}$  distance. As revealed by the X-ray structure (Figure 8), the geometry and arrangement allow pyridyl groups from different  $\text{PD}'\text{O}^-$  units to interdigitate, i.e., a pyridyl group from one  $\text{PD}'\text{O}^-$  moiety lies 'between' two pyridyls from the other  $\text{PD}'\text{O}^-$  group. By contrast, due to greater  $\text{Cu}\cdots\text{Cu}$  distance enforced by the  $\mu$ -1,2-cyanide bridging in **7** connectivity {compared to a  $\mu$ -1,1-Cu–O(H)–Cu linkage}, the intermolecular  $\text{Cu}\cdots\text{Cu}$  distance in **7** is 5.02 Å. The copper(II) ions in **7** adopt square pyramidal geometries with  $\tau$  values of 0.08 and 0.41, respectively.

As mentioned above,  $\text{Cu}^{\text{II}}_2-\text{OOH}$  species may decay to binuclear phenoxo and hydroxo-bridged dinuclear copper(II) complexes, as previously elucidated in the chemistry established for **1A** and **1B**.<sup>14,16</sup> However, such an intramolecular OH-bridged complex is unlikely to form due to the large  $\text{Cu}\cdots\text{Cu}$  distance expected, as in **3**.<sup>32</sup> Formation of the di-hydroxo-bridged complex intramolecular structure with the  $\text{PD}'\text{O}^-$  ligand becomes a good alternative, and the stable species **8** forms.

Complex **8** might also function as the precursor of cyanide-bridged complex **7**. If a concentrated  $\text{EtCN}$  solution of **1** was employed in the syntheses, the green-colored complex **8** would precipitate first after the thermal decay reaction. However, it partly turned blue after 3 or 4 days, indicating the production of **7** occurs. If this solution is then evaporated and the resulting solid recrystallized from  $\text{CH}_3\text{CN}/\text{Et}_2\text{O}$  at ambient temperature, it always gives **7** but not **8**. As indicated in Figure 4, we suggest that compound **8** slowly reacts with  $\text{HCN}$  produced by the hydroxylated nitrile oxidation chemistry by **1** and converts itself to a more stable complex, **7**.

## Summary/Conclusions

Employing a phenol-containing binucleating ligand  $\text{PD}'\text{OH}$ , we can generate the hydroperoxo-dicopper(II) species **1** in

(79) The other possible reaction during this process is the occurrence of a chlorine substitution reaction, as  $^-\text{OH}$  is a strong base. The yielded  $\text{Cl}^-$  subsequently serves as the external ligand for the copper ions.

solution by reacting its dicopper(I) analogue with O<sub>2</sub>. Compared to its structural analogues, the different rigid nature of PD'OH mediates new chemistry: (1) Formation of **1** requires the assistance of a nitrile solvent to coordinate, resulting N<sub>bridgehead</sub> de-ligation enables the copper ions to move closer together to form a  $\mu$ -1,1-(<sup>-</sup>O<sub>2</sub>H) structure. (2) Synthesis of **1** by reacting H<sub>2</sub>O<sub>2</sub> with the corresponding dicopper(II) complex does not work due to the large Cu...Cu distance in the precursor **3**; instead, a (Cu-OOH)<sub>2</sub> species, **4**, forms. (3) The phenolate-bridged Cu(I) complex with PD'OH ligand disproportionates immediately upon an attempted synthesis. (4) Compound **1** thermal decay also leads to a hydroxide-copper(II) product. However, in place of the production of an *intramolecular* hydroxo-bridged dinuclear copper(II) complex, a *intermolecular* di- $\mu$ -OH-bridged tetranuclear copper complex, **8**, is isolated.

The most striking new chemistry comes from the solvent and ligand oxidation reactions which occur during the compound **1** thermal decay process. As previously detailed, decomposition of **1** leads to nitrile solvent hydroxylation, which subsequently decays to yield an aldehyde, releasing cyanide. An apparent  $k_H/k_D = 2.9 \pm 0.2$  isotope effect suggests that  $\alpha$ -H-atom abstraction from the nitrile solvent to yield a corresponding organic radical is likely to be the

first step of the reaction.<sup>30</sup> Here, we described how in a separate process occurring during the thermal decay of **1**, the PD'O<sup>-</sup> ligand is transformed to a Schiff base complex, **6**, apparently having undergone an oxidative N-dealkylation, subsequent oxidative dehydrogenation, and a presumably separate solvent CH<sub>2</sub>Cl<sub>2</sub> chloride extraction. In a process which also involves ligand radical intermediates, a ligand cross-linked product, **5**, forms when a large excess of PPh<sub>3</sub> is added to **1**. These multiple solvent and ligand oxidation reactions explain the lack of external substrate oxidation by **1**.

Clearly, dicopper(II)-hydroperoxides possess a rich substrate oxidative chemistry,<sup>18,30</sup> Future research will include efforts to delineate differences in mononuclear Cu<sup>II</sup>-OOH versus dinuclear Cu<sup>II</sup><sub>2</sub>-OOH structures and reactivity, and attempts to design systems which do not undergo ligand degradation but rather effect only exogenous substrate oxidative transformations.

**Supporting Information Available:** Crystallographic structural data and various spectroscopic data. This material is available free of charge via the Internet at <http://pubs.acs.org>.

IC060598X